Do land surface models need to include differential plant species responses to drought? Examining model predictions across a mesic-xeric gradient in Europe.

M. G. De Kauwe[1], S.-X. Zhou[1,2], B. E. Medlyn[1,3], A. J. Pitman[4], Y.-P. Wang[5], R. A. Duursma[3] and I. C. Prentice[1,6]

[1]{Macquarie University, Department of Biological Sciences, New South Wales 2109, Australia.}

[2] {CSIRO Agriculture Flagship, Waite Campus, PMB 2, Glen Osmond, SA 5064, Australia.}

[3]{Hawkesbury Institute for the Environment, Western Sydney University, Locked Bag 1797, Penrith, NSW, Australia}

[4]{Australian Research Council Centre of Excellence for Climate Systems Science and Climate Change Research Centre, UNSW, Sydney, Austraila}

[5]{CSIRO Ocean and Atmosphere Flagship, Private Bag #1, Aspendale, Victoria 3195, Australia}

[6]{AXA Chair of Biosphere and Climate Impacts, Grand Challenges in Ecosystems and the Environment and Grantham Institute – Climate Change and the Environment, Department of Life Sciences, Imperial College London, Silwood Park Campus, Buckhurst Road, Ascot SL5 7PY, UK}

Correspondence to: M. G. De Kauwe (mdekauwe@gmail.com)

Abstract

Future climate change has the potential to increase drought in many regions of the globe, making it essential that land surface models (LSMs) used in coupled climate models, realistically capture the drought responses of vegetation. Recent data syntheses show that drought sensitivity varies considerably among plants from different climate zones, but state-of-the-art LSMs currently assume the same drought sensitivity for all vegetation. We tested whether variable drought sensitivities are needed to explain the observed large-scale patterns of drought impact on the carbon, water and energy fluxes. We implemented data-driven drought sensitivities in the Community Atmosphere Biosphere Land Exchange (CABLE) LSM and evaluated alternative sensitivities across a latitudinal gradient in Europe during the 2003 heatwave. The model predicted an overly abrupt onset of drought unless average soil water potential was calculated with dynamic weighting across soil layers. We found that high drought sensitivity at the most mesic sites, and low drought sensitivity at the most xeric sites, was necessary to accurately model responses during drought. Our results indicate that LSMs will over-estimate drought impacts in drier climates unless different sensitivity of vegetation to drought is taken into account.

1 Introduction

Changes in regional precipitation patterns with climate change are highly uncertain (Sillmann et al. 2014), but are widely expected to result in a change in the frequency, duration and severity of drought events (Allen et al. 2010). Drought is broadly defined, but for plants is a marked deficit of moisture in the root zone which results from a period of low rainfall and/or increased atmospheric demand for evapotranspiration. Recently, a series of high-profile drought events (Ciais et al. 2005; Fensham et al. 2009; Phillips et al. 2009; Lewis et al. 2011) and associated tree mortality (Breshears et al. 2005; van Mantgem et al. 2009; Peng et al. 2011; Anderegg et al. 2013), have occurred across the globe and these events have led to debate as to whether incidence of drought are increasing (Allen et al. 2010; Dai et al. 2013, but see Sheffield et al. 2012). Drought and any ensuing vegetation mortality events have the potential to change land ecosystems from a sink to source (Lewis et al. 2011), and the dominant mechanisms governing the ecosystem responses to drought can vary from reducing stomatal conductance (Xu and Baldocchi, 2003) to increasing tree mortality (Lewis et al. 2011) and changing community species composition (Nepstad et al. 2007).

Our ability to model drought effect on vegetation function (carbon and water fluxes) is currently limited (Galbraith et al. 2010; Egea et al. 2011; Powell et al. 2013). Remarkably, given the importance of correctly capturing drought impacts on carbon and water fluxes, land surface models (LSMs) designed for use in climate models have rarely been benchmarked against extreme drought events. Mahfouf et al. (1996) compared summertime crop transpiration from 14 land surface schemes, finding that only half of the models fell within the uncertainty range of the observations. They attributed differences among models to the various schemes used by models to represent transpiration processes (e.g. soil water stress function, different number of soil layers) and variability in the initial soil water content at the start of the growing season which relates to variability in the way bare soil evaporation and drainage are represented among different models. Galbraith et al. (2010) showed that a set of dynamic global vegetation models (DGVMs) were unable to capture the 20–30% reduction in biomass due to drought during a set of throughfall exclusion experiments in the Amazon. Galbraith et al. (2010) attributed model variability during drought to: changes in autotrophic respiration (which was not supported by the data), model insensitivity to observed leaf area reductions, and the use of different empirical functions to down-regulate productivity during

water stress. The models differed both in terms of time-scale of the application of this function (sub-diurnal vs. daily) and whether it was used to down-regulate net photosynthesis or the maximum rate of Rubisco activity, V_{cmax}. Similarly, Powell et al. (2013) demonstrated that a group of five models were unable to predict drought-induced reductions in aboveground biomass (~20%) in two large-scale Amazon experiments. Gerten et al. (2008) compared the effect of adjusting precipitation regimes on simulated net primary productivity (NPP) by four ecosystem models across a range of hydroclimates. They found a consistent direction of change (in terms of NPP) with different scenarios across models but found that the seasonal evolution of soil moisture differed among the models.

In order for models to better capture realistic responses during drought, they need to draw more closely on experimental data (see Chaves et al. 1993 for a review). One key observation is that there is a continuum of species responses to soil moisture deficit, ranging from isohydric (stomata close rapidly during drought, maintaining a minimum leaf water potential, Ψ_l) to anisohydric (stomata remain open during drought, which allows Ψ_l to decrease) hydraulic strategies (Tardieu and Simonneau, 1998; Klein, 2014). These differences are widely observed and are thought to be important in determining resilience to drought (McDowell et al. 2008; Mitchell et al. 2013; Garcia-Forner et al. 2015). Many traits, including hydraulic conductivity, resistance to cavitation, turgor loss point, stomatal regulation and rooting depth, contribute to these differences. Systematic differences in the response of leaf gas exchange to soil moisture potential have been observed among species originating from different hydroclimates (Zhou et al. 2013), with species from mesic environments showing stronger stomatal sensitivity to drought than species from xeric environments. Currently, these environmental gradients in species behaviour are not captured in LSMs, which typically assume static plant functional type (PFT) parameterisations. This is in part because historically the data required to describe these attributes have not been available at the global scale, but also due to the necessity of simplification required to run global climate model simulations. Species with a PFT are assumed to have similar or identical sensitivities to drought. Such an approach ignores experimental evidence of the range of sensitivities to drought among species (Choat et al. 2012; Limousin et al. 2013; Zhou et al. 2014; Mitchell et al., 2014; Mencuccini et al. 2015). For example, Turner et al. (1984) found contrasting responses in leaf water potential to increasing vapour pressure deficit, ranging from isohydric

to anisohydric, among a group of woody and herbaceous species. Similarly, Zhou et al. (2014) found that in a dry-down experiment, European sapling species originating from more mesic environments were more sensitive to water stress (more rapid reduction of photosynthesis and stomatal conductance) than species from more xeric regions. However, it is not known whether observed differences in the response to soil moisture deficit among species are important in determining fluxes at large scales.

In this study we test whether differences in species' responses to drought are needed to capture drought responses on a continental scale. We built on recent changes to the stomatal conductance (g_s) scheme (De Kauwe et al. 2015) within the Community Atmosphere Biosphere Land Exchange (CABLE) LSM (Wang et al. 2011), by implementing a new formulation for drought impacts based on plant ecophysiological studies for 31 species (Zhou et al. 2013; 2014). We obtained three parameterisations for drought response from these studies, characterising low, medium and high sensitivities to drought. We then applied CABLE to simulate responses to an extreme meteorological event, the European 2003 heatwave, at five eddy covariance sites covering a latitudinal gradient, transitioning from mesic sites at the northern extreme to xeric at the southern sites. Observations show that there was a significant impact of drought on ecosystem fluxes at these sites (Ciais et al. 2005; Schär et al. 2005). We note that models have been applied to simulate drought effects on productivity (net primary production) and leaf area at individual sites (Ciais et al. 2005; Fischer et al. 2007; Granier et al. 2007; Reichstein et al. 2007) but have not been used to examine whether alternative parameterisations are needed to capture drought responses across sites. We therefore tested how well CABLE was able to simulate the impact of drought on carbon and water fluxes at these sites using alternative parameterisations for drought sensitivity. We hypothesised that drought sensitivity would increase as sites transitioned from xeric to mesic. We hypothesised that trees at more mesic sites, with a greater abundance of available water than at xeric sites, would be more vulnerable to shorter duration droughts, and thus have higher drought sensitivity (or lower resistance to drought). Therefore, accounting for this latitudinal gradient in drought sensitivity would improve the performance of CABLE.

2 Methods

2.1 Model description

CABLE represents the vegetation using a single layer, two-leaf canopy model separated into sunlit and shaded leaves (Wang and Leuning, 1998), with a detailed treatment of within canopy turbulence (Raupach 1994; Raupach et al. 1997). Soil water and heat conduction is numerically integrated over six discrete soil layers following the Richards equation and up to three layers of snow can accumulate on the soil surface. A complete description can be found in Kowalczyk et al. (2006) and Wang et al. (2011). CABLE has been used extensively for both offline (Abramowitz et al. 2008; Wang et al. 2011; De Kauwe et al. 2015) and coupled simulations (Cruz et al. 2010; Pitman et al. 2011; Mao et al. 2011; Lorenz et al. 2014) within the Australian Community Climate Earth System Simulator (ACCESS, see http://www.accessimulator.org.au; Kowalczyk et al. 2013); a fully coupled earth system model. The source code can be accessed after registration at https://trac.nci.org.au/trac/cable.

2.2 Representing drought stress within CABLE.

We build on the work by De Kauwe et al. (2015), who introduced a new g_s scheme into CABLE. In this scheme, stomata are assumed to behave optimally; that is, stomata are regulated to maximise carbon gain whilst simultaneously minimising water loss, over short time periods (i.e. a day) (Cowan and Farquhar, 1977) leading to the following formulation of g_s (Medlyn et al. 2011)

$$g_s = g_0 + 1.6\left(1 + \frac{g_1}{\sqrt{D}}\right)\frac{A}{C_s} \quad (1)$$

where A is the net assimilation rate (μmol m^{-2} s^{-1}), C_s (μmol mol^{-1}) and D (kPa) are the CO_2 concentration and the vapour pressure deficit at the leaf surface, respectively, and g_0 (mol m^{-2} s^{-1}), and g_1 are fitted constants representing the residual stomatal conductance when A reaches zero, and the slope of the sensitivity of g_s to A, respectively. The model was parameterised for different PFTs using data from Lin et al. (2015) (see De Kauwe et al. 2015).

In the standard version of CABLE, drought stress is implemented as an empirical scalar (β) that depends on soil moisture content, weighted by the fraction of roots in each of CABLE's six soil layers:

$$\beta = \sum_{i=1}^{n} f_{root,i} \frac{\theta_i - \theta_w}{\theta_{fc} - \theta_w};\ \beta \in [0,1] \quad (2)$$

where θ_i is the volumetric soil moisture content ($m^3\ m^{-3}$) in soil layer i, θ_w is the wilting point ($m^3\ m^{-3}$), θ_{fc} is the field capacity ($m^3\ m^{-3}$) and $f_{root,i}$ is the fraction of root mass in soil layer i. The six soil layers in CABLE have depths 0.022 m, 0.058 m, 0.154 m, 0.409 m, 1.085 m and 2.872 m. The factor β is assumed to limit the slope of the relationship between stomatal conductance (g_s, mol $m^{-2}\ s^{-1}$; Leuning 1995) by acting as a modifier on the parameter g_1.

In this study, we introduced a new expression for drought sensitivity of gas exchange, based on the work of Zhou et al. (2013, 2014). In this model, both g_1 and the photosynthetic parameters V_{cmax} and J_{max} are assumed to be sensitive to pre-dawn leaf water potential, but this sensitivity varies across species. There is considerable evidence that both g1 and V_{cmax} are sensitive to soil moisture (Keenan et al. 2009; Egea et al. 2011; Flexas et al. 2012; Zhou et al. 2013). There is also widespread evidence that plants are more directly respond to water potential rather than water content (Comstock and Mencuccini 1998; Verhoef and Egea, 2014).

Zhou et al. (2013) extended the optimal stomatal model of Medlyn et al. (2011) by fitting an exponential function to relate g_1 to pre-dawn leaf water potential (Ψ_{pd}):

$$g_1 = g_{1wet} \times \exp(b\Psi_{pd}) \quad (3)$$

where g_{1wet} is fitted parameter representing plant water use under well watered conditions (i.e. when $\Psi_{pd} = 0$) and b is a fitted parameter representing the sensitivity of g_1 to Ψ_{pd}. Species with different water use strategies can by hypothesised to differ in not only their g_1 parameter under well-watered conditions, g_{1wet} (see Lin et al. 2015), but also with the sensitivity to Ψ_{pd}, b. Zhou et al. (2013) also advanced a non-stomatal limitation to the photosynthetic biochemistry, which describes the apparent effect of water stress on V_{cmax}:

$$V_{cmax} = V_{cmax,wet} \frac{1 + \exp(S_f \Psi_f)}{1 + \exp(S_f (\Psi_f - \Psi_{pd}))} \quad (4)$$

where $V_{cmax,wet}$ is the V_{cmax} value in well watered conditions, S_f is a sensitivity parameter describing the steepness of the decline with water stress, Ψ_f is the water potential at which Ψ_{pd} decreases to half of its maximum value. As with g_1, it is hypothesised that in the same way species vary in their V_{cmax} values in well-watered conditions ($V_{cmax,wet}$), they would also differ in their sensitivity of down-regulated V_{cmax} with water stress (Zhou et al. 2014). In CABLE, as there is a constant ratio between the parameters J_{max} and V_{cmax}, the parameter J_{max} is similarly reduced by drought.

To implement Eq. (6) in CABLE we first had to convert soil moisture content (θ) to pre-dawn leaf water potential (Ψ_{pd}). We did so by assuming that overnight Ψ_{pd} and Ψ_S equilibrate before sunrise, thus ignoring any night-time transpiration (Dawson et al. 2007). Following Campbell (1974), we related θ to Ψ_S in each soil layer by:

$$\Psi_{S,i} = \Psi_e \left(\frac{\theta_i}{\theta_{sat}}\right)^{-k} \quad (5)$$

where Ψ_e is the air entry water potential (MPa) and k (unitless) is an empirical coefficient which is related to the soil texture. Values for Ψ_e and b are taken from CABLE's standard lookup table following Clapp and Hornberger (1978). We then needed to obtain a representative weighted estimate of Ψ_S across CABLE's soil layers. We tested three potential approaches for weighting in this paper:

(i) Using the root-biomass weighted θ and converting this to Ψ_S using Eq. (8), hereafter denoted M1. Such an approach is often favoured by models, following experimental evidence that plants preferentially access regions in the root zone where water is most freely available (Green and Clotheir 1995; Huang et al. 1997).

(ii) Taking the integrated θ over the top 5 soil layers (1.7 m depth) and converting this to Ψ_S using Eq. (8), hereafter denoted M2. This method assumes the plant effectively has access to an entire "bucket" of soil water. This approach is often favoured by "simpler" forest productivity models (e.g. Landsberg and Waring, 1997).

(iii) Weighting the average Ψ_S for each of the six soil layers by the weighted soil-to-root conductance to water uptake of each layer, following Williams et al. (1996; 2001), hereafter denoted M3. The total conductance term depends the combination of a soil component (R_s) and a root component (R_r). R_s is defined as (Gardner, 1960):

$$R_s = \frac{\ln\left(\frac{r_s}{r_r}\right)}{2\pi l_r D G_{soil}} \quad (6)$$

where r_s is the mean distance between roots (m), r_r is the fine root radius (m), D is the depth of the soil layer, G_{soil} is the soil conductivity (mmol m^{-1} s^{-1} MPa^{-1}) which depends on soil texture and soil water content, l_r is the fine root density (mm^{-3}). R_r is defined as:

$$R_r = \frac{R_r^*}{FD} \quad (7)$$

where R_r^* is the root resistivity (MPa s g $mmol^{-1}$), F is the root biomass per unit volume (g m^{-3}). This method weights Ψ_S to the upper soil layers when the soil is wet, but shifts towards layer lowers as the soil dries, due to the lower soil hydraulic conductance (e.g. Duursma et al. 2011).

2.3 Model simulations

During 2003, Europe experienced an anomalously dry summer, amplified by a combination of a preceding dry spring and high summer temperatures (Ciais et al. 2005; Schär et al. 2005). Summer temperatures were recorded to have exceeded the 30-year June-July-August (JJA) average by 3°C (Schär et al. 2005). Consequently we choose to focus our model comparisons on this period, in particular the period between June and September 2003.

At each of the five Fluxnet sites we ran three sets of simulations:

- A control simulation ("CTRL"), representing CABLE version 2.0.1.
- Three simulations to explore the new drought model using a "high" (*Quercus robur*), "medium" (*Quercus ilex*) and "low" (*Cedrus atlantica*) sensitivity to soil moisture.

Parameter values were obtained from the meta-analysis by Zhou et al. (2013; 2014) and are given in Table 1. For each of these simulations we also tested the three different methods of obtaining Ψ_S as described above.

- A "no drought" simulation in which any transpired water was returned to the soil. By comparing this simulation with either the control or any of the new drought model simulations (high, medium, low), a guide to the magnitude of the drought should be apparent.

Model parameters were not calibrated to match site characteristics; instead default PFT parameters were used for each site. Although CABLE has the ability to simulate full carbon, nitrogen and phosphorus biogeochemical cycling, this feature was not activated for this study, instead only the carbon and water cycle were simulated. For all simulations, leaf area index (LAI) was prescribed using CABLE's gridded monthly LAI climatology derived from Moderate-resolution Imaging Spectroradiometer (MODIS) LAI data (Knyazikhin et al. 1998; 1999) and the g_s scheme following Medlyn et al. (2011; see De Kauwe et al. 2015) was used throughout. All model simulations were spun-up by repeating the meteorological forcing site data until soil moisture and soil temperatures reached equilibrium (as we were ignoring the full biogeochemical cycling in these simulations).

2.4 Datasets used

To assess the performance of the CABLE model both with and without the new drought scheme, we selected a gradient of five forested Fluxnet (http://www.fluxdata.org/) sites across Europe (Table 2) from those available through the Protocol for the Analysis of Land Surface models (PALS; pals.unsw.edu.au; Abramowitz, 2012). These data have previously been pre-processed and quality controlled for use within the LSM community. Consequently, all site-years had near complete observations of key meteorological drivers (as opposed to significant gap-filled periods).

Model simulations were compared to measured latent heat and flux-derived gross primary productivity (GPP) at each of the FLUXNET sites. Flux-derived GPP estimates are calculated

from the measured net ecosystem exchange (NEE) of carbon between the atmosphere and the vegetation/soil, and the modelled ecosystem respiration (R_{eco}), where GPP is calculated as NEE + R_{eco}.

3 Results

Severity of the 2003 drought

Table 3 summarises summer differences in rainfall, air temperature, GPP and LE between 2002 and 2003 across the five sites covering the latitudinal gradient from mesic to xeric sites across Europe. Whilst the impact of the 2003 heatwave varied between sites, every site was warmer and drier in 2003. Similarly, GPP was lower at every site except Espirra, and LE was lower at three of the sites (Hesse, Roccarespampani and Castelporziano) in 2003 than in 2002.

Simulated fluxes during drought from the standard model

Figure 1 shows a site-scale comparison between standard CABLE (CTRL) transpiration (E), flux derived GPP, and the observed LE at the five sites. Table 4 and 5 shows a series of summary statistics (Root Mean Squared Error (RMSE), Nash-Sutcliffe efficiency (NSE), Pearsons's correlation coefficient (r) between modelled and observed GPP and LE. An indication of the severity of the drought can be obtained by comparing the difference between the "No drought" and the CTRL simulation.

For the two more mesic sites (Tharandt and Hesse), the CTRL simulation generally matched the trajectory of the observed LE, but displayed systematic periods of over-estimation (i.e. under-estimated the drought effect). By contrast, in the three more xeric sites (Roccarespampani, Castelporziano and Espirra), the reverse was true: the CTRL simulations descended into drought stress much more quickly than the observed fluxes. This rapid drought progression was particularly evident around day of year 155 at the Roccarespampani site. Across all sites, agreement with observed LE fluxes was generally poor (RMSE = 21.25 W m^{-2} to 38 W m^{-2}; NSE = –8.95 to 0.15). This outcome is partly a result of the high soil evaporation around mid-spring, which results in CABLE simulating very large LE fluxes during this period.

At Tharandt, Hesse and Roccarespampani, simulated GPP systematically underestimated the flux-derived peak GPP, particularly evident before day of year 180. Transitioning to the more xeric sites (Roccarespampani, Castelporziano and Espirra), simulated GPP was apparently too

sensitive to water stress, contributing to a poor agreement with flux-derived data (RMSE = 2.22 g C m^{-2} to 3.03 g C m^{-2}; NSE = –2.67 to 0.42).

Theoretical behaviour of new drought scheme

We now consider the implementation of the new drought model and the three sensitivity parameterisations. Figure 2a shows how leaf-level photosynthesis is predicted to decline (using Eqs. 3 and 4) in the new drought model with increasing water stress (more negative Ψ_S). The different sensitivities to drought are clearly visible, with the three parameterisations representing a spectrum of behaviour ranging from high to low drought sensitivity. Figures 2b and c show how the new drought model compares to the standard CABLE (CTRL; using Eq. 2) model on a sandy and clay soil type. The CTRL model is seen to most closely match the high sensitivity simulation on a sandy soil, but it predicts an earlier descent into drought stress. By contrast on the clay soil, the new medium and high sensitivity simulations encompass the predictions from the CTRL model. The new drought model and parameterisations afford a more flexible sensitivity to the down-regulation of photosynthesis with drought, which is particularly evident in the low sensitivity simulation.

Impact of new drought scheme on modelled LE

Figures 3–7 show the same site comparisons as Fig. 1, but with the addition of the new drought model and the three different ways (M1-3) in which Ψ_S can be averaged over the soil profile. Across all sites it is clear that using M1, the new drought model behaves in much the same way as the CTRL simulation. The explanation is that weighting Ψ_S by the fraction of roots in each layer, results in water being principally extracted from the top three shallow layers (Supplementary figures S1–S5). Consequently, small changes in θ result in a rapid decline in Ψ_S (owing to the non-linear relationship between θ and Ψ_S, Fig. 1), which causes an unrealistically abrupt shutdown of transpiration. M2 showed a greater separation between the three sensitivity parameterisations than method one. The greater separation is most evident at the xeric sites; the model performs particularly well at Espirra (LE RMSE < 16 W m^{-2} vs. CTRL RMSE = 35.31 W m^{-2}) and to a lesser extent at Castelporziano (LE low sensitivity RMSE = 19.72 W m^{-2} vs. CTRL RMSE = 31.76 W m^{-2}) (Table 4). Nevertheless, at the two mesic sites, the model completely underestimates the size of the drought, as a result of

using a large soil water bucket (1.7 m) to calculate Ψ_S. M3 in combination with the new drought model generally performed the best across all the sites, as it allows CABLE to simulate a more gradual reduction of fluxes during drought. At Roccarespampani a medium drought sensitivity performed best at reproducing the observed LE (CTRL RMSE = 38.0 W m^{-2} vs. 18.27 W m^{-2}), whilst at Espirra (CTRL RMSE = 35.31 W m^{-2} vs. 15.40 W m^{-2}) the low sensitivity performed best (Table 4). At Castelporziano, both low (CTRL RMSE = 31.76 W m^{-2} vs. 20.41 W m^{-2}) and medium sensitivity (LE RMSE = 20.47 W m^{-2}) performed well (Table 4). In contrast, at the two mesic sites, a high drought sensitivity performed best, although at both Hesse (LE CTRL RMSE = 21.25 W m^{-2} vs. 25.90 W m^{-2}) and Tharandt (LE CTRL RMSE = 28.5 W m^{-2} vs. 28.82 W m^{-2}), the new drought model performed marginally worse than the CTRL (Table 4).

Impact of new drought scheme on modelled GPP

At the more xeric sites, there were noticeable improvements in simulated GPP during the drought period (Figures 3–7). Similar to the LE result, across all sites M3 worked best (Table 5): using a medium drought sensitivity at both Roccarespampani (CTRL RMSE = 2.49 g C m^{-2} d^{-1} vs. 1.73 g C m^{-2} d^{-1}) and Castelporziano (CTRL RMSE = 2.22 g C m^{-2} d^{-1} vs. 0.95 g C m^{-2} d^{-1}), and a low sensitivity at Espirra (CTRL RMSE = 3.03 g C m^{-2} d^{-1} vs. 1.43 g C m^{-2} d^{-1}). At the mesic end of the gradient, a medium sensitivity at Hesse (CTRL RMSE = 2.85 g C m^{-2} d^{-1} vs. 2.71 g C m^{-2} d^{-1}) and a medium or high sensitivity at Tharandt worked best; although using either sensitivity performed slightly worse than the CTRL (CTRL RMSE = 2.06 g C m^{-2} d^{-1} vs. >= 2.23 g C m^{-2} d^{-1}) (Table 5).

4 Discussion

Experimental data suggest that plants exhibit a continuum of drought sensitivities, with species originating in more mesic environments showing higher sensitivity than species from more xeric environments (Bahari et al. 1985; Reich and Hinckley, 1989; Ni and Pallardy, 1991; Zhou et al. 2014). We investigated whether variable drought sensitivity improves the ability of the CABLE LSM to reproduce observed drought impacts across a latitudinal gradient. We found that, at the mesic sites, a high drought sensitivity was required; moving southwards towards more xeric sites, the sensitivity parameterisation transitioned to a medium and finally to a low drought sensitivity. Whilst this characterisation of the transition of drought sensitivities was largely consistent for both water and carbon fluxes, it is notable for the two most mesic sites, a medium rather than a high drought sensitivity performed best for carbon fluxes. There are a number of possible explanations; however, as the relationships tested are not site-specific it is hard to be conclusive as to the exact cause. Nevertheless, it does suggest that the parameterisation of the high drought sensitivity may be too sensitive at mesic sites, which will need further investigation. This work demonstrates the importance of understanding how plant traits vary with climate across the landscape. However, our analysis also highlighted the importance of identifying which soil layers matter most to the plant: our results depended strongly on how we weighted soil moisture availability through the profile.

Weighting soil moisture availability

Commonly, empirical dependences of gas exchange on soil moisture content or potential (Eqns 3, 4) are estimated from pot experiments (e.g. Zhou et al. 2013; 2014), in which it is fair to assume that the soil moisture content is relatively uniform and fully explored by roots. In contrast, soil moisture content and rooting depth in the field typically have strong vertical profiles. Thus, to implement such equations in a land surface model requires that we specify how to weight the soil layers to obtain a representative value of whole-profile θ or Ψ_S. In this study we tested three potential implementations. Our first approach was to weight each layer by root biomass. Evidence suggests that plants preferentially access regions in the root zone where water is most freely available (Green and Clotheir 1995; Huang et al. 1997). Hence, many models follow this approach: for example, the original version of CABLE weighted soil moisture content by root biomass (Eqn 2) while the Community Land Model (CLM)

estimates a water stress factor based on a root-weighted Ψ_S, using a PFT-defined minimum and maximum water potential (Oleson et al. 2013). However, we found that this approach performed poorly. We observed an 'on-off' behaviour in response to drought, which occurs because the behaviour of the model is driven by the top soil layers, whose total soil moisture content is relatively small and root biomass is relatively high, and can be depleted rapidly, leading to a sudden onset of severe drought. Many other LSMs show this abrupt effect of drought (Egea et al., 2011; Powell et al., 2013). Powell et al. (2013) found that four models (CLM version 3.5, Integrated BIosphere Simulator version 2.6.4 (IBIS), Joint UK Land Environment Simulator version 2.1 (JULES), and Simple Biosphere model version 3 (SiB3)) implement abrupt transitions of this kind. We also found that with this weighting of soil layers, there was little effect of variable drought sensitivity: the depletion of soil moisture content of the top layers is so rapid that there is little difference between low and high sensitivities to drought. Such an outcome suggests that there is little adaptive significance of drought sensitivity, which seems unlikely. A further implication of using a root-weighted function to calculate Ψ_S is that two distinctly different scenarios, a soil that has been very wet but experienced a short dry period, allowing the topsoil to dry, and a soil that has had a prolonged period of drought but experienced a recent rainfall event, would have similar impacts on gas exchange. Again, this outcome seems unlikely.

We tested a second implementation in which soil moisture potential was calculated from the moisture content of the entire rooting zone (top five soil layers = 1.7 m). Such an approach is commonly used in forest productivity models (e.g. Landsberg and Waring, 1997). However, this approach severely underestimates drought impacts because the moisture content of the total soil profile is so large, meaning that it is rarely depleted enough to impact on gas exchange.

In reality, plant water uptake shifts lower in the profile as soil dries out (e.g. Duursma et al. 2011). Thus, in our third implementation, we tested an approach in which the weighting of soil layers moves downwards as drought progresses. This approach is effectively similar to that used by the soil–plant–atmosphere (SPA) model (Williams et al. 1996; 2001), in which soil layers are weighted by their soil-to-root conductance, which declines as the moisture

content declines. Of the three approaches we tested, this method performed best, allowing CABLE to replicate the observations across the latitudinal mesic to xeric gradient. This dynamic weighting of Ψ_S may partially explain previous good performance by SPA in other model inter-comparisons focussed on drought (e.g. Powell et al. 2013). Recently, Bonan et al. (2014) tested the suitability of using a model that considers optimal stomatal behaviour and plant hydraulics (SPA; Williams et al. 1996) for earth system modelling, and demonstrated marked improvement over the standard model during periods of drought stress. We thus suggest that models using a soil moisture stress function to simulate drought effects on gas exchange should consider a dynamic approach to weighting the contribution of different soil layers.

We note that this issue is related to another long-standing problem for LSMs: that of determining the vertical distribution of root water uptake (e.g. Feddes et al., 2001; Federer et al., 2003; Kleidon and Heimann, 1998, 2000). In the standard version of CABLE, water uptake from each soil layer initially depends on the fraction of root biomass in each layer, but moves downwards during drought as the upper layers are depleted. It is possible that changes to the weighting of soil moisture in determining drought sensitivity should also be accompanied by changes to the distribution of root water uptake, but we did not explore this option here. Li et al. (2012) previously tested an alternative dynamic root water uptake function (Lai and Katul, 2000) in CABLE, but found little improvement in predicted LE during seasonal droughts without also considering a mechanism for hydraulic redistribution. Further work should evaluate models not only against LE fluxes, but also against measurements of soil moisture profiles. Many experimental sites now routinely install multiple soil moisture sensors (e.g. direct gravimetric sampling, neutron probes, time domain reflectometry), which provide accurate insight into root water extraction and hydraulic redistribution, even down to considerable depths (>4 m). These data have thus far been underutilised for model improvement, but should be a priority for reducing the uncertainty in soil moisture dynamics.

Incorporating different sensitivities to drought

476 Using the third and best method to calculate overall Ψ_s, we found that varying drought
477 sensitivity across sites enabled the model to better capture drought effects across the
478 mesic/xeric gradient, with a high drought sensitivity implied in mesic sites and a low drought
479 sensitivity implied in xeric sites. These results should not be surprising, given the increasing
480 amount of experimental evidence suggesting that drought sensitivity varies among species
481 and across climates (e.g. Engelbrecht and Kursar, 2003; Engelbrecht et al. 2007; Skelton et al.
482 2015). In contrast to these data, most LSMs assume a single parameterisation for drought
483 sensitivity, which is typically based on mesic vegetation. Our results suggest that such a
484 parameterisation is very likely to overstate the impacts of drought on both carbon and water
485 fluxes in drier regions.
486
487 Our work thus underlines a need to move beyond models that implement drought sensitivity
488 through a single PFT parameterisation. Although we only compared vegetation at five sites, it
489 has been widely shown that species originating from different hydroclimates vary in their
490 drought sensitivities (Choat et al. 2012; Limousin et al. 2013; Zhou et al. 2014; Mitchell et al.,
491 2014; Mencuccini et al. 2015) and our results indicate that these differing sensitivities at the
492 plant level are also important at the ecosystem scale. It is, of course, challenging to implement
493 such a continuum of sensitivities in a global vegetation model. In this study, we used a simple
494 site-specific approach in which we selected three sets of model parameters from a meta-
495 analysis by Zhou et al. (2013; 2014), allowing us to characterise a range of plant responses to
496 drought. The approach we tested in this paper could not be directly implemented in global
497 vegetation models: these models would require a more sophisticated approach that relates
498 drought sensitivity to the climate of each pixel. One potential solution would be to develop an
499 empirical correlation between drought sensitivity and a long-term moisture index (e.g. the
500 ratio of mean precipitation to the equilibrium evapotranspiration; Cramer and Prentice, 1988;
501 Gallego-Sala et al. 2010). Previous studies have demonstrated the feasibility of linking model
502 parameters that determine plant water use strategy to such a moisture index in global
503 simulations (Wang et al. 2014; De Kauwe et al. 2015). Such an approach would requires a
504 concerted effort to collate appropriate data, as there are few compilations to date of traits
505 related to drought sensitivity (but see Manzoni et al. 2011; Zhou et al. 2013). Another, more
506 challenging, alternative, would be to develop optimization hypotheses that can predict
507 vegetation drought sensitivity from climate (e.g. Manzoni et al. 2014).

508

509 *Further model uncertainties*

510 Whilst this work advances the ability of LSMs to simulate drought, it does not address all
511 processes needed to correctly capture drought impacts. Other issues to consider include: (i)
512 rooting depth; (ii) leaf shedding; (iii) soil evaporation; and (iv) soil heterogeneity, among
513 others.

514

515 Here we have assumed that all sites had the soil depth (4.6 m), with rooting depth distributed
516 exponential through the profile, as is commonly used in LSMs. However, this assumption
517 may be incorrect. Access to water by deep roots could be a potential alternative explanation
518 for the low drought sensitivity that we inferred at the southernmost (xeric) site, Espirra. Here
519 the dominant species is not native to the region, but rather a plantation of blue gum
520 (*Eucalyptus globulus*), a species that is generally found to have high, not low, drought
521 sensitivity (White 1996; Mitchell et al. 2014). Many eucalypts have a deep rooting strategy
522 (Fabiao et al. 1987), suggesting a possible alternative explanation for drought tolerance at this
523 site. More in-depth study of fluxes and soil moisture patterns at this site would be needed to
524 determine the role of rooting depth.

525

526 During droughts, plants are often observed to shed their leaves. This is a self-regulatory
527 mechanism to reduce water losses (Tyree et al. 1993; Jonasson et al. 1997; Bréda et al. 2006).
528 During the 2003 heatwave at Hesse, an early reduction of approximately 1.7 m^2 m^{-2} was
529 observed. Similarly, at Brasschaat there was a observed reduction of 0.8 m^2 m^{-2} and at
530 Tharandt needle-litter was increased during September until November, with LAI estimated to
531 be 0.9 m^2 m^{-2} lower (Bréda et al. 2006; Granier et al. 2007). In contrast, models typically fix
532 turnover rates for leaves and as such this feedback is largely absent from models. During
533 periods of water stress, models do simulate an indirect reduction in LAI via down-regulated
534 net primary productivity, but this feedback is much slower than is commonly observed. Not
535 accounting for this canopy-scale feedback will result in models over-estimating carbon and
536 water fluxes and thus losses in θ during drought.

537

538 Existing models also disagree as to the mechanism by which to down-regulate productivity
539 during periods of water stress (De Kauwe et al. 2013). In the standard version of CABLE,
540 only the slope of the relationship between g_s and A is reduced by water stress. The SPA model
541 behaves similarly. In contrast, JULES (Clark et al. 2011) and the Sheffield Dynamic Global
542 Vegetation Model (SDGVM; Woodward and Lomas, 2004), down-regulate the
543 photosynthetic capacity via the biochemical parameters V_{cmax} and J_{max} (maximum electron
544 transport rate). Here, we assumed that water stress affects both the slope of g_s-A and the
545 biochemical parameters V_{cmax} and J_{max}, supported by results from Zhou et al. (2013, 2014).
546 We did not evaluate this assumption against the eddy flux data. However, previous studies
547 have also suggested that both effects are needed to explain responses of fluxes during drought
548 (Keenan et al. 2010).

549

550 Finally, although models do have the capacity to simulate vertical variations in θ, they do not
551 always represent horizontal sub-grid scale variability. This assumption is likely to contribute
552 to the abruptness of modelled transitions from well-watered to completely down-regulated
553 carbon and water fluxes. Earlier work by Entekhabi and Eagleson (1989), and models such as
554 the variable infiltration capacity (VIC) model (Liang et al. 1994), and most recently Decker
555 2015 (submitted) have attempted to address this issue by employing statistical distributions to
556 approximate horizontal spatial heterogeneity in soil moisture (see also Crow and Wood,
557 2002). These parsimonious approaches typically require few parameters, making them
558 attractive in the LSM context and potentially suitable for modelling ecosystem and
559 hydrological responses to drought (Luo et al. 2013).

560

561 *Testing models against extreme events*

562 In conclusion, we have used a model evaluation against flux measurements during a large-
563 scale heatwave event to make significant progress in modelling of drought impacts. While
564 model evaluation against data is now commonplace (Prentice et al. 2015) and has recently
565 been extended to formal benchmarking, particularly in the land surface community
566 (Abramowitz, 2005; Best et al. 2015), many of these benchmarking indicators are based on
567 seasonal or annual outputs and thus miss the opportunity to examine model performance
568 during extreme events. Model projections under future climate change require good

569 mechanistic representations of the impacts of extreme events. However, responses to extreme
570 events are rarely evaluated and there is therefore an urgent need to orient model testing to
571 periods of extremes. To that end, precipitation manipulation experiments (e.g. Nepstad et al.
572 2002; Hanson et al. 2003; Pangle et al. 2012) represent a good example of a currently under-
573 exploited avenue (but see Fisher et al. 2007; Powell et al. 2013) that could be used for model
574 evaluation and/or benchmarking (Smith et al. 2014). However, we urge that these exercises do
575 not focus solely on overall model performance, but also test the realism of individual model
576 assumptions (Medlyn et al. 2015).
577
578
579
580
581
582
583
584
585
586
587
588
589
590
591
592
593
594
595

Acknowledgements

This work was supported by the Australian Research Council (ARC) Linkage grant LP140100232 and the ARC Centre of Excellence for Climate System Science (CE110001028). SZ was supported by an international Macquarie University Research Excellence Scholarship. This work is also a contribution to the AXA Chair Programme in Biosphere and Climate Impacts and the Imperial College initiative on Grand Challenges in Ecosystems and the Environment. We thank CSIRO and the Bureau of Meteorology through the Centre for Australian Weather and Climate Research for their support in the use of the CABLE model. This work used eddy covariance data acquired by the FLUXNET community for the La Thuile FLUXNET release, supported by the following networks: AmeriFlux (U.S. Department of Energy, Biological and Environmental Research, Terrestrial Carbon Program (DE-FG02-04ER63917 and DE-FG02-04ER63911)), AfriFlux, AsiaFlux, CarboAfrica, CarboEuropeIP, CarboItaly, CarboMont, ChinaFlux, Fluxnet-Canada (supported by CFCAS, NSERC, BIOCAP, Environment Canada, and NRCan), GreenGrass, KoFlux, LBA, NECC, OzFlux, TCOS-Siberia, USCCC. We acknowledge the financial support to the eddy covariance data harmonization provided by CarboEuropeIP, FAO-GTOS-TCO, iLEAPS, Max Planck Institute for Biogeochemistry, National Science Foundation, University of Tuscia, Université Laval and Environment Canada and US Department of Energy and the database development and technical support from Berkeley Water Center, Lawrence Berkeley National Laboratory, Microsoft Research eScience, Oak Ridge National Laboratory, University of California - Berkeley, University of Virginia. All data analysis and plots were generated using the Python language and the Matplotlib plotting library (Hunter, 2007).

626 **References**

627 Abramowitz, G.: Towards a benchmark for land surface models, Geophys. Res. Lett., 32,
628 L22702, 2005.

629

630 Abramowitz, G.: Towards a public, standardized, diagnostic benchmarking system for land
631 surface models, Geosci. Model Dev., 5, 819–827, 2012.

632

633 Abramowitz, G., Leuning, R., Clark, M. and Pitman, A.: Evaluating the Performance of Land
634 Surface Models, J. Clim., 21, 5468–5481, 2008.

635

636 Allen, C. D., Macalady, A. K., Chenchouni, H., Bachelet, D., McDowell, N., Vennetier, M.,
637 Kitzberger, T., Rigling, A., Breshears, D. D., Hogg, E. H. (Ted), Gonzalez, P., Fensham, R.,
638 Zhang, Z., Castro, J., Demidova, N., Lim, J.-H., Allard, G., Running, S. W., Semerci, A. and
639 Cobb, N.: A global overview of drought and heat-induced tree mortality reveals emerging
640 climate change risks for forests, For. Ecol. Manag., 259, 660–684, 2010.

641

642 Anderegg, W. R., Kane, J. M. and Anderegg, L. D.: Consequences of widespread tree
643 mortality triggered by drought and temperature stress, Nat. Clim. Change, 3, 30–36, 2013.

644

645 Bahari, Z. A., Pallardy, S. G. and Parker, W.C. Photosynthesis, water relations, and drought
646 adaptation in six woody species of oak-hickory forests in central Missouri. For. Sci. 31:557-
647 569, 1985.

648

649 Best, M. J., Abramowitz, G., Johnson, H. R., Pitman, A. J., Balsamo, G. and Boone, A.,
650 Cuntz, M., Decharme, B., Dirmeyer, P. A., Dong, J., Ek, M., Guo, Z., Haverd, V., van den
651 Hurk, B. J. J., Nearing, G. S., Pak, B., Peters-Lidard, C., Santanello Jr., J. A., Stevens, L. and
652 Vuichard, N.: The Plumbing of Land Surface Models: Benchmarking Model Performance. J.
653 Hydrometeor, 16, 1425–1442, 2015.

654

655 Bonan, G., Williams, M., Fisher, R. and Oleson, K.: Modeling stomatal conductance in the
656 Earth system: linking leaf water-use efficiency and water transport along the soil-plant-
657 atmosphere continuum, Geosci. Model Dev., 7, 2193–2222, 2014.

658

659 Bréda, N., Huc, R., Granier, A. and Dreyer, E.: Temperate forest trees and stands under severe
660 drought: a review of ecophysiological responses, adaptation processes and long-term
661 consequences, Ann. For. Sci., 63, 625–644, 2006.

662

663 Breshears, D. D., Cobb, N. S., Rich, P. M., Price, K. P., Allen, C. D., Balice, R. G., Romme,
664 W. H., Kastens, J. H., Floyd, M. L., Belnap, J., Anderson, J. J., Myers, O. B. and Meyer, C.
665 W.: Regional vegetation die-off in response to global-change-type drought, Proc. Natl. Acad.
666 Sci. U. S. A., 102, 15144–15148, 2005.

667

668 Campbell, G. S.: A simple method for determining unsaturated conductivity from moisture
669 retention data., Soil Sci., 117, 311–314, 1974.

670

671 Canadell, J., Jackson, R., Ehleringer, J., Mooney, H., Sala, O. and Schulze, E.-D.: Maximum
672 rooting depth of vegetation types at the global scale, Oecologia, 108, 583–595, 1996.

673

674 Chaves, M. M., Maroco, J. P. and Pereira, J. S.: Understanding plant responses to drought—
675 from genes to the whole plant, Funct. Plant Biol., 30, 239–264, 2003.

676

677 Choat, B., Jansen, S., Brodribb, T. J., Cochard, H., Delzon, S., Bhaskar, R., Bucci, S. J., Feild,
678 T. S., Gleason, S. M., Hacke, U. G., Jacobsen, A. L., Lens, F., Maherali, H., Martinez-Vilalta,
679 J., Mayr, S., Mencuccini, M., Mitchell, P. J., Nardini, A., Pittermann, J., Pratt, R. B., Sperry,
680 J. S., Westoby, M., Wright, I. J. and Zanne, A. E.: Global convergence in the vulnerability of
681 forests to drought, Nature, 491, 752–755, 2012.

682

683 Ciais, P., Reichstein, M., Viovy, N., Granier, A., Ogee, J., Allard, V., Aubinet, M.,
684 Buchmann, N., Bernhofer, C., Carrara, A., Chevallier, F., De Noblet, N., Friend, A. D.,
685 Friedlingstein, P., Grunwald, T., Heinesch, B., Keronen, P., Knohl, A., Krinner, G., Loustau,

686 D., Manca, G., Matteucci, G., Miglietta, F., Ourcival, J. M., Papale, D., Pilegaard, K.,
687 Rambal, S., Seufert, G., Soussana, J. F., Sanz, M. J., Schulze, E. D., Vesala, T. and Valentini,
688 R.: Europe-wide reduction in primary productivity caused by the heat and drought in 2003,
689 Nature, 437, 529–533, 2005.

690

691 Clapp, R. B. and Hornberger, G. M.: Empirical equations for some soil hydraulic properties,
692 Water Resour. Res., 14, 601–604, 1978.

693

694 Clark, D. B., Mercado, L. M., Sitch, S., Jones, C. D., Gedney, N., Best, M. J., Pryor, M.,
695 Rooney, G. G., Essery, R. L. H., Blyth, E., Boucher, O., Harding, R. J., Huntingford, C. and
696 Cox, P. M.: The Joint UK Land Environment Simulator (JULES), model description - Part 2:
697 Carbon fluxes and vegetation dynamics, Geosci. Model Dev., 4, 701–722, 2011.

698

699 Comstock, J. and Mencuccini, M.: Control of stomatal conductance by leaf water potential in
700 Hymenoclea salsola (T. & G.), a desert subshrub, Plant Cell Environ., 21, 1029–1038, 1998.

701

702 Cowan, I. and Farquhar, G.: Stomatal function in relation to leaf metabolism and
703 environment., in Society for Experimental Biology Symposium, Integration of Activity in the
704 Higher Plant, vol. 31, edited by D. H. Jennings, pp. 471–505, Cambridge University Press.,
705 1977.

706

707 Cramer, W. and Prentice, I.: Simulation of regional soil moisture deficits on a European scale,
708 Nor. Geogr. Tidsskr. - Nor. J. Geogr., 42, 149–151, 1988.

709

710 Crow, W. T and Wood, E. F.: Impact of soil moisture aggregation on surface energy flux
711 prediction during SGP'97. Geophys. Res. Lett., 29. 8-1, 2002.

712

713 Cruz, F. T., Pitman, A. J. and Wang, Y.-P.: Can the stomatal response to higher atmospheric
714 carbon dioxide explain the unusual temperatures during the 2002 Murray-Darling Basin
715 drought?, J. Geophys. Res. Atmospheres, 115(D2), 2010.

716
717 Dai, A.: Increasing drought under global warming in observations and models, Nat. Clim.
718 Change, 3, 52–58, 2013.
719
720 Dawson, T. E., Burgess, S. S., Tu, K. P., Oliveira, R. S., Santiago, L. S., Fisher, J. B.,
721 Simonin, K. A. and Ambrose, A. R.: Nighttime transpiration in woody plants from contrasting
722 ecosystems, Tree Physiol., 27, 561–575, 2007.
723
724 Decker, M., A new Soil Moisture and Runoff Parameterization for the CABLE LSM
725 including subgrid scale processes, J. Adv. Model Earth Sy., submitted, 2015.
726
727 De Kauwe, M. G., Medlyn, B. E., Zaehle, S., Walker, A. P., Dietze, M. C., Hickler, T., Jain,
728 A. K., Luo, Y., Parton, W. J., Prentice, I. C., Smith, B., Thornton, P. E., Wang, S., Wang, Y.-
729 P., Waarlind, D., Weng, E., Crous, K. Y., Ellsworth, D. S., Hanson, P. J., Seok Kim, H.-,
730 Warren, J. M., Oren, R. and Norby, R. J.: Forest water use and water use efficiency at
731 elevated CO_2: a model-data intercomparison at two contrasting temperate forest FACE sites,
732 Glob. Change Biol., 19, 1759–1779, 2013.
733
734 De Kauwe, M. G., Kala, J., Lin, Y.-S., Pitman, A. J., Medlyn, B. E., Duursma, R. A.,
735 Abramowitz, G., Wang, Y.-P. and Miralles, D. G.: A test of an optimal stomatal conductance
736 scheme within the CABLE land surface model, Geosci. Model Dev., 8, 431–452, 2015.
737
738 Duursma, R., Kolari, P., Perämäki, M., Nikinmaa, E., Hari, P., Delzon, S., Loustau, D.,
739 Ilvesniemi, H., Pumpanen, J. and Mäkelä, A.: Predicting the decline in daily maximum
740 transpiration rate of two pine stands during drought based on constant minimum leaf water
741 potential and plant hydraulic conductance, Tree Physiol., 28, 265–276, 2008.
742
743 Duursma, R. A., Barton, C. V. M., Eamus, D., Medlyn, B. E., Ellsworth, D. S., Forster, M. A.,
744 Tissue, D. T., Linder S., McMurtrie, R. E. Rooting depth explains $[CO_2] \times$ drought interaction
745 in Eucalyptus saligna. Tree Physiol., 31, 922–931, 2011.
746

747 Egea, G., Verhoef, A. and Vidale, P. L.: Towards an improved and more flexible
748 representation of water stress in coupled photosynthesis–stomatal conductance models, Agric.
749 For. Meteorol., 151, 1370–1384, 2011.

750

751 Engelbrecht, B. M. J., Comita, L. S., Condit, R., Kursar, T. A., Tyree, M. T., Turner, B. L.,
752 Hubbell, S. P.: Drought sensitivity shapes species distribution patterns in tropical forests.
753 Nature, 447, 80-82.

754 Engelbrecht, B. M. J. and Kursar, T. A. Comparative drought-resistance of seedlings of 28
755 species of co-occurring tropical woody plants. Oecologia, 136, 383–393, 2003.

756

757 Entekhabi, D. and Eagleson, P. S.: Land surface hydrology parameterization for atmospheric
758 general circulation models including subgrid scale spatial variability, J. Clim., 2, 816–831,
759 1989.

760

761 Fabião A., Madeira M., Steen E.: Root mass in plantations of Eucalyptus globulus in Portugal
762 in relation to soil characteristics. Arid Soil Res. Rehabil 1, 185-194, 1987.

763

764 Feddes, R. A., Hoff, H., Bruen, M., Dawson, T., de Rosnay, P., Dirmeyer, P., Jackson, R. B.,
765 Kabat, P., Kleidon, A., Lilly, A. and Pitman, A. J.: Modeling root water uptake in
766 hydrological and climate models, Bull. Am. Meteorol. Soc., 82, 2797–2809, 2001.

767

768 Federer, C., Vörösmarty, C. and Fekete, B.: Sensitivity of annual evaporation to soil and root
769 properties in two models of contrasting complexity, J. Hydrometeorol., 4, 1276–1290, 2003.

770

771 Fensham, R., Fairfax, R. and Ward, D.: Drought-induced tree death in savanna, Glob. Change
772 Biol., 15, 380–387, 2009.

773

774 Fischer, E., Seneviratne, S., Lüthi, D. and Schär, C.: Contribution of land-atmosphere
775 coupling to recent European summer heat waves, Geophys. Res. Lett., 34, 2007.

776

777 Flexas, J., Barbour, M. M., Brendel, O., Cabrera, H. M., Carriquí, M., Díaz-Espejo, A.,
778 Douthe, C., Dreyer, E., Ferrio, J. P., Gago, J., Gallé, A., Galmés, J., Kodama, N., Medrano,
779 H., Niinemets, Ü., Peguero-Pina, J. J., Pou, A., Ribas-Carbó, M., Tomás, M., Tosens, T. and
780 Warren, C. R.: Mesophyll diffusion conductance to CO_2: an unappreciated central player in
781 photosynthesis, Plant Sci., 193, 70–84, 2012.

782

783 Galbraith, D., Levy, P. E., Sitch, S., Huntingford, C., Cox, P., Williams, M. and Meir, P.:
784 Multiple mechanisms of Amazonian forest biomass losses in three dynamic global vegetation
785 models under climate change, New Phytol., 187, 647–665, 2010.

786

787 Gallego-Sala, A., Clark, J., House, J., Orr, H., Prentice, I. C., Smith, P., Farewell, T. and
788 Chapman, S.: Bioclimatic envelope model of climate change impacts on blanket peatland
789 distribution in Great Britain, Clim. Res., 45, 151–162, 2010.

790

791 Garcia-Forner, N., Adams, H. D., Sevanto, S., Collins, A. D., Dickman, L. T., Hudson, P. J.,
792 Zeppel, M., Martínez-Vilalta, J. and Mcdowell, N. G.: Responses of two semiarid conifer tree
793 species to reduced precipitation and warming reveal new perspectives for stomatal regulation,
794 Plant Cell Amp Environ., in press, 2015.

795

796 Gerten, D., Luo, Y., Le Maire, G., Parton, W. J., Keough, C., Weng, E., Beier, C., Ciais, P.,
797 Cramer, W., Dukes, J. S., Hanson, P. J., Knapp, A. A. K., Linder, S., Nepstad, D., Rustad, L.
798 and Sowerby, A.: Modelled effects of precipitation on ecosystem carbon and water dynamics
799 in different climatic zones, Glob. Change Biol., 14, 2365–2379, 2008.

800

801 Green, S. R. and Clothier, B. E.: Root water uptake by kiwifruit vines following partial
802 wetting of the root zone. Plant Soil, 173, 317-328, 1995.

803

804 Hanson, P. J., M. A. Huston, and D. E. Todd: Walker branch throughfall displacement
805 experiment, in North American Temperate Deciduous Forest Responses to Changing

806 Precipitation Regimes, edited by P. J. Hanson and S. D. Wullschleger, pp. 8–31, Springer,
807 New York, 2003.
808
809 Huang, B., R. R. Duncan, and R. N. Carrow (1997), Drought-resistance mechanisms of seven
810 warm-season turfgrasses under surface soil drying: II. Root aspects, Crop Sci., 37, 1863–
811 1869.
812
813 Hunter, J. D.: Matplotlib: A 2D graphics environment, Comput. Sci. Amp Eng., 9, 90–95,
814 2007.
815
816 Keenan, T., García, R., Friend, A., Zaehle, S., Gracia, C. and Sabate, S.: Improved
817 understanding of drought controls on seasonal variation in Mediterranean forest canopy CO_2
818 and water fluxes through combined in situ measurements and ecosystem modelling,
819 Biogeosciences, 6, 1423–1444, 2009.
820
821 Keenan, T., Sabate, S. and Gracia, C.: The importance of mesophyll conductance in
822 regulating forest ecosystem productivity during drought periods, Glob. Change Biol., 16,
823 1019–1034, 2010.
824
825 Kleidon, A. and Heimann, M.: A method of determining rooting depth from a terrestrial
826 biosphere model and its impacts on the global water and carbon cycle, Glob. Change Biol., 4,
827 275–286, 1998.
828
829 Klein, T.: The variability of stomatal sensitivity to leaf water potential across tree species
830 indicates a continuum between isohydric and anisohydric behaviours, Funct. Ecol., 28, 1313–
831 1320, 2014.
832
833 Knyazikhin, Y., Marshak, J. V., Diner, D. J., B, M. R., Verstraete, M., B, P. and Gobron, N.:
834 Estimation of vegetation canopy leaf area index and fraction of absorbed photosynthetically

active radiation from atmosphere-corrected MISR data, J. Geophys. Res., 103, 32239–32257, 1998.

Knyazikhin, Y., Glassy, J., Privette, J. L., Tian, Y., Lotsch, A., Zhang, Y., Wang, Y., Morisette, J. T., P.Votava, Myneni, R. B., Neman, R. R. and Running, S. W.: MODIS Leaf Area Index (LAI) and Fraction of Photosynthetically Active Radiation Absorbed by Vegetation (FPAR) Product (MOD15) Algorithm Theoretical Basis Document. [online] Available from: http://eospso.gsfc.nasa.gov/atbd/modistables.html, 1999.

Kowalczyk, E., Stevens, L., Law, R., Dix, M., Wang, Y., Harman, I., Haynes, K., Srbinovsky, J., Pak, B. and Ziehn, T.: The land surface model component of ACCESS: description and impact on the simulated surface climatology, Aust Meteorol Ocean. J, 63, 65–82, 2013.

Kowalczyk, E. A., Wang, Y. P., Wang, P., Law, R. H. and Davies, H. L.: The CSIRO Atmosphere Biosphere Land Exchange (CABLE) model for use in climate models and as an offline model, CSIRO, 2006.

Lai, C. T. and Katul, G.: The dynamic role of root-water uptake in coupling potential to actual transpiration, Adv. Water Resour., 23, 427–439, 2000.

Landsberg, J. and Waring, R.: A generalised model of forest productivity using simplified concepts of radiation-use efficiency, carbon balance and partitioning, For. Ecol. Manag., 95, 209–228, 1997.

Leuning, R.: A critical appraisal of a combined stomatal-photosynthesis model for C_3 plants., Plant Cell Environ., 18, 339–355, 1995.

Lewis, S. L., Brando, P. M., Phillips, O. L., van der Heijden, G. M. and Nepstad, D.: The 2010 amazon drought, Science, 331, 554–554, 2011.

Li, L., Wang, Y.-P., Yu, Q, Pak, B., Eamus, D., Yan, J., van Gorsel, E. and Baker, I. T.: Improving the responses of the Australian community land surface model (CABLE) to seasonal drought. J. Geophys. Res-Biogeo., 117, G4, 2012.

Liang, X., Lettenmaier, D. P., Wood, E. F. and Burges, S. J.: A simple hydrologically based model of land surface water and energy fluxes for general circulation models, J. Geophys. Res.- Ser.-, 99, 14–415, 1994.

Limousin, J.-M., Bickford, C. P., Dickman, L. T., Pangle, R. E., Hudson, P. J., Boutz, A. L., Gehres, N., Osuna, J. L., Pockman, W. T. and McDowell, N. G.: Regulation and acclimation of leaf gas exchange in a piñon–juniper woodland exposed to three different precipitation regimes, Plant Cell Environ., 36, 1812–1825, 2013.

Lin, Y.-S., Medlyn, B. E., Duursma, R. A., Prentice, I. C., Wang, H., Baig, S., Eamus, D., de Dios, V. R., Mitchell, P., Ellsworth, D. S., de Beeck, M. O., Wallin, G., Uddling, J., Tarvainen, L., Linderson, M.-L., Cernusak, L. A., Nippert, J. B., Ocheltree, T. W., Tissue, D. T., Martin-StPaul, N. K., Rogers, A., Warren, J. M., De Angelis, P., Hikosaka, K., Han, Q., Onoda, Y., Gimeno, T. E., Barton, C. V. M., Bennie, J., Bonal, D., Bosc, A., Low, M., Macinins-Ng, C., Rey, A., Rowland, L., Setterfield, S. A., Tausz-Posch, S., Zaragoza-Castells, J., Broadmeadow, M. S. J., Drake, J. E., Freeman, M., Ghannoum, O., Hutley, L. B., Kelly, J. W., Kikuzawa, K., Kolari, P., Koyama, K., Limousin, J.-M., Meir, P., Lola da Costa, A. C., Mikkelsen, T. N., Salinas, N., Sun, W. and Wingate, L.: Optimal stomatal behaviour around the world, Nat. Clim. Change, 5, 459–464, 2015.

Lorenz, R., Pitman, A., Donat, M., Hirsch, A., Kala, J., Kowalczyk, E., Law, R. and Srbinovsky, J.: Representation of climate extreme indices in the ACCESS1. 3b coupled atmosphere-land surface model, Geosci. Model Dev., 7, 545–567, 2014.

Luo, X., Liang, X., and McCarthy, H. R.: VIC+ for water-limited conditions: a study of biological and hydrological processes and their interactions in the soil-plant-atmosphere continuum, Water Resour. Res., 49, 7711-7732, 2013.

Mahfouf, J.-F., Ciret, C., Ducharne, A., Irannejad, P., Noilhan, J., Shao, Y., Thornton, P., Xue, Y. and Yang, Z.-L.: Analysis of transpiration results from the RICE and PILPS workshop, Glob. Planet. Change, 13, 73–88, 1996.

Manzoni, S.: Integrating plant hydraulics and gas exchange along the drought-response trait spectrum. Tree Physiol, 34, 1031-1034, 2014.

Manzoni, S., Vico, G., Katul, G., Fay, P. A., Polley, W., Palmroth, S. and Porporato, A. Optimizing stomatal conductance for maximum carbon gain under water stress: a meta-analysis across plant functional types and climates. Funct. Ecol., 25, 456-467, 2011.

Mao, J., Pitman, A. J., Phipps, S. J., Abramowitz, G. and Wang, Y.: Global and regional coupled climate sensitivity to the parameterization of rainfall interception, Clim. Dyn., 37, 171–186, 2011.

McDowell, N., Pockman, W. T., Allen, C. D., Breshears, D. D., Cobb, N., Kolb, T., Plaut, J., Sperry, J., West, A., Williams, D. G. and others: Mechanisms of plant survival and mortality during drought: why do some plants survive while others succumb to drought?, New Phytol., 178, 719–739, 2008.

McDowell, N. G. and Allen, C. D.: Darcy's law predicts widespread forest mortality under climate warming, Nat. Clim. Change, 5, 669–672, 2015.

Medlyn, B. E. and Zaehle, S. and De Kauwe, M. G. and Walker, A. P. and Dietze, M. C. and Hanson, P. J. and Hickler, T. and Jain, A. K. and Luo, Y. and Parton, W. and Prentice, I. C. and Thornton, P. E. and Wang, S. and Wang, Y.-P. and Weng, E. and Iversen, C. M. and McCarthy, H. R. and Warren, J. M. and Oren, R. and Norby, R. J.: Using ecosystem experiments to improve vegetation models. Nature Clim. Change, 5, 528-534, 2015.

926 Medlyn, B. E., Duursma, R. A., Eamus, D., Ellsworth, D. S., Prentice, I. C., Barton, C. V. M.,
927 Crous, K. Y., De Angelis, P., Freeman, M. and Wingate, L.: Reconciling the optimal and
928 empirical approaches to modelling stomatal conductance, Glob. Change Biol., 17, 2134–2144,
929 2011.
930
931 Mencuccini, M., Minunno, F., Salmon, Y., Martínez-Vilalta, J. and Hölttä, T.: Coordination
932 of physiological traits involved in drought-induced mortality of woody plants, New Phytol., in
933 press, 2015.
934
935 Milly, P.: Sensitivity of greenhouse summer dryness to changes in plant rooting
936 characteristics, Geophys. Res. Lett., 24, 269–271, 1997.
937
938 Mitchell, P., O'Grady, A., Tissue, D., Worledge, D. and Pinkard, E.: Co-ordination of growth,
939 gas exchange and hydraulics define the carbon safety margin in tree species with contrasting
940 drought strategies, Tree Physiol., 34, 443–458, 2014.
941
942 Mitchell, P. J., O'Grady, A. P., Tissue, D. T., White, D. A., Ottenschlaeger, M. L. and
943 Pinkard, E. A.: Drought response strategies define the relative contributions of hydraulic
944 dysfunction and carbohydrate depletion during tree mortality, New Phytol., 197, 862–872,
945 2013.
946
947 Nepstad, D. C., Tohver, I. M., Ray, D., Moutinho, P. and Cardinot, G.: Mortality of large
948 trees and lianas following experimental drought in an Amazon forest, Ecology, 88, 2259–
949 2269, 2007.
950
951 Nepstad, D. C. and Moutinho, P. and Dias-Filho, M. B. and Davidson, E. and Cardinot, G.
952 and Markewitz, D. and Figueiredo, R. and Vianna, N. and Chambers, J. and Ray, D. and
953 Guerreiros, J. B. and Lefebvre, P. and Sternberg, L. and Moreira, M. and Barros, L. and
954 Ishida, F. Y. and Tohlver, I. and Belk, E. and Kalif, K. and Schwalbe, K.: The effects of
955 partial throughfall exclusion on canopy processes, aboveground production, and
956 biogeochemistry of an Amazon forest, J. Geophys. Res., 107(D20), 8085, 2156-2202, 2002.

Ni, B.-R., and S. G. Pallardy. Response of gas exchange to water stress in seedlings of woody angiosperms. Tree Physiol., 8, 1–9, 1991.

Oleson, K. W., Lawrence, D. M., Bonan, G. B., Drewniak, B., Huang, M., Koven, C. D., Levis, S., Li, F., Riley, W. J., Subin, Z. M., Swenson, S. C., Thornton, P. E., Bozbiyik, A., Fisher, R., Heald, C. L., Kluzek, E., Lamarque, J.-F., Lawrence, P. J., Leung, L. R., Lipscomb, W., Muszala, S., Ricciuto, D. M., Sacks, W., Sun, Y., Tang, J. and Yang, Z.-L.: Technical Description of version 4.5 of the Community Land Model (CLM), NCAR Technical Note, Citeseer, National Center for Atmospheric Research, P.O. Box 3000, Boulder, Colarado., 2013.

Pangle, R. E., J. P. Hill, J. A. Plaut, E. A. Yepez, J. R. Elliot, N. Gehres, N. G. McDowell, and W. T. Pockman: Methodology and performance of a rainfall manipulation experiment in a piñon–juniper woodland, Ecosphere, 3, art28, 2012.

Peng, C., Ma, Z., Lei, X., Zhu, Q., Chen, H., Wang, W., Liu, S., Li, W., Fang, X. and Zhou, X.: A drought-induced pervasive increase in tree mortality across Canada's boreal forests, Nat. Clim. Change, 1, 467–471, 2011.

Phillips, O. L., Aragão, L. E. O. C., Lewis, S. L., Fisher, J. B., Lloyd, J., López-González, G., Malhi, Y., Monteagudo, A., Peacock, J., Quesada, C. A., van der Heijden, G., Almeida, S., Amaral, I., Arroyo, L., Aymard, G., Baker, T. R., Bánki, O., Blanc, L., Bonal, D., Brando, P., Chave, J., de Oliveira, Á. C. A., Cardozo, N. D., Czimczik, C. I., Feldpausch, T. R., Freitas, M. A., Gloor, E., Higuchi, N., Jiménez, E., Lloyd, G., Meir, P., Mendoza, C., Morel, A., Neill, D. A., Nepstad, D., Patiño, S., Peñuela, M. C., Prieto, A., Ramírez, F., Schwarz, M., Silva, J., Silveira, M., Thomas, A. S., Steege, H. ter, Stropp, J., Vásquez, R., Zelazowski, P., Dávila, E. A., Andelman, S., Andrade, A., Chao, K.-J., Erwin, T., Di Fiore, A., C., E. H., Keeling, H., Killeen, T. J., Laurance, W. F., Cruz, A. P., Pitman, N. C. A., Vargas, P. N., Ramírez-Angulo, H., Rudas, A., Salamão, R., Silva, N., Terborgh, J. and Torres-Lezama, A.: Drought sensitivity of the Amazon rainforest, Science, 323, 1344–1347, 2009.

Pitman, A., Avila, F., Abramowitz, G., Wang, Y., Phipps, S. and de Noblet-Ducoudré, N.: Importance of background climate in determining impact of land-cover change on regional climate, Nat. Clim. Change, 1, 472–475, 2011.

Powell, T. L., Galbraith, D. R., Christoffersen, B. O., Harper, A., Imbuzeiro, H. M. A., Rowland, L., Almeida, S., Brando, P. M., da Costa, A. C. L., Costa, M. H., Levine, N. M., Malhi, Y., Saleska, S. R., Sotta, E., Williams, M., Meir, P. and Moorcroft, P. R.: Confronting model predictions of carbon fluxes with measurements of Amazon forests subjected to experimental drought, New Phytol., 200, 350–365, 2013.

Raupach, M.: Simplified expressions for vegetation roughness length and zero-plane displacement as functions of canopy height and area index, Bound.-Layer Meteorol., 71, 211–216, 1994.

Raupach, M., Finkele, K. and Zhang, L.: SCAM (Soil-Canopy-Atmosphere Model): Description and comparison with field data, Aspendale Aust. CSIRO CEM Tech. Rep., (132), 81, 1997.

Reich, P. B. and T. M. Hinckley. Influence of pre-dawn water potential and soil-to-leaf hydraulic conductance on maximum daily leaf diffusive conductance in two oak species. Funct. Ecol. 3:719-126, 1989.

Reichstein, M., Ciais, P., Papale, D., Valentini, R., Running, S., Viovy, N., Cramer, W., Granier, A., Ogée, J., Allard, V., Aubinet, M., Bernhofer, C., Buchmann, N., Carrara, A., Grünwald, T., Heimann, M., Heinesch, B., Knohl, A., Kutsch, W., Loustau, D., Manca, G., Matteucci, G., Miglietta, F., Ourcival, J. M., Pilegaard, K., Pumpanen, J., Rambal, S., Schaphoff, S., Seufert, G., Soussana, J.-F., Sanz, M.-J., Vesala, T. and Zhao, M.: Reduction of ecosystem productivity and respiration during the European summer 2003 climate anomaly: a joint flux tower, remote sensing and modelling analysis, Glob. Change Biol., 13, 634–651, 2007.

1019 Schär, C., Vidale, P. L., Lüthi, D., Frei, C., Häberli, C., Liniger, M. A. and Appenzeller, C.:
1020 The role of increasing temperature variability in European summer heatwaves, Nature, 427,
1021 332–336, 2004.
1022
1023 Sheffield, J., Wood, E. F. and Roderick, M. L.: Little change in global drought over the past
1024 60 years, Nature, 491, 435–438, 2012.
1025
1026 Skelton, R. P., West, A. G. and Dawson, T. E.: Predicting plant vulnerability to drought in
1027 biodiverse regions using functional traits, 112, 5744-5749, 2015.
1028
1029 Smith, N. G., Rodgers, V. L., Brzostek, E. R., Kulmatiski, A., Avolio, M. L., Hoover, D. L.,
1030 Koerner, S. E., Grant, K., Jentsch, A. and Fatichi, S., Niyogi, D.: Toward a better integration
1031 of biological data from precipitation manipulation experiments into Earth system models,
1032 Rev. of Geophys., 52, 1944-9208, 2014.
1033
1034 Tardieu, F. and Simonneau, T.: Variability among species of stomatal control under
1035 fluctuating soil water status and evaporative demand: modelling isohydric and anisohydric
1036 behaviours, J. Exp. Bot., 49, 419–432, 1998.
1037
1038 Tyree, M., Cochard, H., Cruiziat, P., Sinclair, B. and Ameglio, T.: Drought-induced leaf
1039 shedding in walnut: evidence for vulnerability segmentation, Plant Cell Environ., 16, 879–
1040 882, 1993.
1041
1042 van Mantgem, P. J., Stephenson, N. L., Byrne, J. C., Daniels, L. D., Franklin, J. F., Fulé, P.
1043 Z., Harmon, M. E., Larson, A. J., Smith, J. M., Taylor, A. H. and others: Widespread increase
1044 of tree mortality rates in the western United States, Science, 323, 521–524, 2009.
1045
1046 Verhoef, A. and Egea, G.: Modeling plant transpiration under limited soil water: Comparison
1047 of different plant and soil hydraulic parameterizations and preliminary implications for their
1048 use in land surface models, Agric. For. Meteorol., 191, 22–32, 2014.
1049

1050 Wang, H., Prentice, I. and Davis, T.: Biophysical constraints on gross primary production by
1051 the terrestrial biosphere, Biogeosciences, 11, 5987–6001, 2014.
1052
1053 Wang, Y. P. and Leuning, R.: A two-leaf model for canopy conductance, photosynthesis and
1054 partitioning of available energy I::: Model description and comparison with a multi-layered
1055 model, Agric. For. Meteorol., 91, 89–111, 1998.
1056
1057 Wang, Y. P., Kowalczyk, E., Leuning, R., Abramowitz, G., Raupach, M. R., Pak, B., van
1058 Gorsel, E. and Luhar, A.: Diagnosing errors in a land surface model (CABLE) in the time and
1059 frequency domains, J. Geophys. Res. Biogeosciences 2005–2012, 116, 2011.
1060
1061 White, D.: Physiological responses to drought of Eucalyptus globulus and Eucalyptus nitens
1062 in plantations. PhD diss., University of Tasmania, 1996.
1063
1064 Williams, M., Rastetter, E. B., Fernandes, D. N., Goulden, M. L., Wofsy, S. C. and Shaver, G.
1065 R. and: Modelling the soil-plant-atmosphere continuum in a Quercus-Acer stand at Harvard
1066 Forest: the regulation of stomatal conductance by light, nitrogen and soil/plant hydraulic
1067 properties., Plant Cell Environ., 19, 911–927, 1996.
1068
1069 Williams, M., Bond, B. and Ryan, M.: Evaluating different soil and plant hydraulic
1070 constraints on tree function using a model and sap flow data from ponderosa pine, Plant Cell
1071 Amp Environ., 24, 679–690, 2001.
1072
1073 Woodward, F. I. and Lomas, M. R.: Vegetation dynamics - simulating responses to climate
1074 change., Biol. Rev., 79, 643–670, 2004.
1075
1076 Xu, L. and Baldocchi, D. D.: Seasonal trends in photosynthetic parameters and stomatal
1077 conductance of blue oak (Quercus douglasii) under prolonged summer drought and high
1078 temperature, Tree Physiol., 23, 865–877, 2003.
1079

Zhou, S., Duursma, R. A., Medlyn, B. E., Kelly, J. W. and Prentice, I. C.: How should we model plant responses to drought? An analysis of stomatal and non-stomatal responses to water stress, Agric. For. Meteorol., 182-183, 204–214, 2013.

Zhou, S., Medlyn, B., Sabaté, S., Sperlich, D. and Prentice, I. C.: Short-term water stress impacts on stomatal, mesophyll and biochemical limitations to photosynthesis differ consistently among tree species from contrasting climates, Tree Physiol., 10, 1035–1046, 2014.

Figure Captions

Figure 1: A comparison of the observed (OBS) and modelled (CTRL) Latent Heat (LE) and transpiration (E) at five Fluxnet sites during 2003. The data have been smoothed with a 5-day moving window to aid visualisation.

Figure 2: Modelled impact of drought on the assimilation rate (A), shown as (a) a function of volumetric soil moisture content (θ) and (b) soil water potential (Ψ_S) for a sand and clay soil.

Figure 3: A comparison of the observed (OBS) and modelled latent Heat (LE), transpiration (E) and gross primary productivity (GPP) at the Tharandt site during 2003. Simulations show the control (CTRL) and the three parameterisations that represent a spectrum of behaviour ranging from a high to low drought sensitivity, and the tested methods to obtain a weighted estimate of soil water potential (Ψ_S) across CABLE's soil layers (M1-M3). M1 uses a root-biomass weighted soil water content converted to Ψ_S, M2 calculates Ψ_S by integrated soil water content over the top 1.7m of the soil, and M3 is calculated using a dynamic weight across soil layers. The data have been smoothed with a 5-day moving window to aid visualisation and the grey bars show daily rainfall.

Figure 4: A comparison of the observed (OBS) and modelled latent Heat (LE), transpiration (E) and gross primary productivity (GPP) at the Hesse site during 2003. Simulations show the control (CTRL) and the three parameterisations that represent a spectrum of behaviour ranging from a high to low drought sensitivity, and the tested methods to obtain a weighted estimate of soil water potential (Ψ_S) across CABLE's soil layers (M1-M3). M1 uses a root-biomass weighted soil water content converted to Ψ_S, M2 calculates Ψ_S by integrated soil water content over the top 1.7m of the soil, and M3 is calculated using a dynamic weight across soil layers. The data have been smoothed with a 5-day moving window to aid visualisation and the grey bars show daily rainfall.

Figure 5: A comparison of the observed (OBS) and modelled latent Heat (LE), transpiration (E) and gross primary productivity (GPP) at the Roccarespampani site during 2003. Simulations show the control (CTRL) and the three parameterisations that represent a spectrum of behaviour ranging from a high to low drought sensitivity, and the tested methods to obtain a weighted estimate of soil water potential (Ψ_S) across CABLE's soil layers (M1-M3). M1 uses a root-biomass weighted soil water content converted to Ψ_S, M2 calculates Ψ_S by integrated soil water content over the top 1.7m of the soil, and M3 is calculated using a dynamic weight across soil layers. The data have been smoothed with a 5-day moving window to aid visualisation and the grey bars show daily rainfall.

Figure 6: A comparison of the observed (OBS) and modelled latent Heat (LE), transpiration (E) and gross primary productivity (GPP) at the Castelporziano site during 2003. Simulations show the control (CTRL) and the three parameterisations that represent a spectrum of behaviour ranging from a high to low drought sensitivity, and the tested methods to obtain a weighted estimate of soil water potential (Ψ_S) across CABLE's soil layers (M1-M3). M1 uses a root-biomass weighted soil water content converted to Ψ_S, M2 calculates Ψ_S by integrated soil water content over the top 1.7m of the soil, and M3 is calculated using a dynamic weight across soil layers. The data have been smoothed with a 5-day moving window to aid visualisation and the grey bars show daily rainfall.

Figure 7: A comparison of the observed (OBS) and modelled latent Heat (LE), transpiration (E) and gross primary productivity (GPP) at the Espirra site during 2003. Simulations show the control (CTRL) and the three parameterisations that represent a spectrum of behaviour ranging from a high to low drought sensitivity, and the tested methods to obtain a weighted estimate of soil water potential (Ψ_S) across CABLE's soil layers (M1-M3). M1 uses a root-biomass weighted soil water content converted to Ψ_S, M2 calculates Ψ_S by integrated soil water content over the top 1.7m of the soil, and M3 is calculated using a dynamic weight across soil layers. The data have been smoothed with a 5-day moving window to aid visualisation and the grey bars show daily rainfall.

Supplementary Figure 1: Simulated soil water content of each of CABLE's six layers for the control (CTRL), and three drought sensitivities (high, medium, low) based on Zhou et al. (2013; 2014) at the Tharandt site. The grey shading highlights the heatwave period between the 1st of June and the 31st of August. The data have been smoothed with a 5-day moving window to aid visualisation.

Supplementary Figure 2: Simulated soil water content of each of CABLE's six layers for the control (CTRL), and three drought sensitivities (high, medium, low) based on Zhou et al. (2013; 2014) at the Hesse site. The grey shading highlights the heatwave period between the 1st of June and the 31st of August. The data have been smoothed with a 5-day moving window to aid visualisation.

Supplementary Figure 3: Simulated soil water content of each of CABLE's six layers for the control (CTRL), and three drought sensitivities (high, medium, low) based on Zhou et al. (2013; 2014) at the Roccarespampani site. The grey shading highlights the heatwave period between the 1st of June and the 31st of August. The data have been smoothed with a 5-day moving window to aid visualisation.

Supplementary Figure 4: Simulated soil water content of each of CABLE's six layers for the control (CTRL), and three drought sensitivities (high, medium, low) based on Zhou et al. (2013; 2014) at the Castelporziano site. The grey shading highlights the heatwave period between the 1st of June and the 31st of August. The data have been smoothed with a 5-day moving window to aid visualisation.

Supplementary Figure 5: Simulated soil water content of each of CABLE's six layers for the control (CTRL), and three drought sensitivities (high, medium, low) based on Zhou et al. (2013; 2014) at the Espirra site. The grey shading highlights the heatwave period between the 1st of June and the 31st of August. The data have been smoothed with a 5-day moving window to aid visualisation.

Table 1. Baseline parameter values used to represent the three sensitivities: "high" (*Quercus robur*), "medium" (*Quercus ilex*) and "low" (*Cedrus atlantica*) to drought stress. Paramater values are taken from Zhou et al. (2013; 2014).

Sensitivity	b	S_f	Ψ_f
High	1.55	6.0	–0.53
Medium	0.82	1.9	–1.85
Low	0.46	5.28	–2.31

Table 2: Summary of flux tower sites.

Site	PFT	Dominant species	Latitude	Longitude	Country	Sand/Silt/Clay Fraction
Tharandt	ENF	*Picea abies*	50°58' N	13°34' E	Germany	0.37/0.33/0.3
Hesse	DBF	*Fagus sylvatica*	48°40' N	7°05' E	France	0.37/0.33/0.3
Roccarespampani	DBF	*Quercus cerris*	42°24' N	11°55' E	Italy	0.6/0.2/0.2
Castelporziano	EBF	*Quercus ilex*	41°42' N	12°22' E	Italy	0.6/0.2/0.2
Espirra	EBF	*Eucalyptus globulus*	38°38' N	8°36' W	Portugal	0.37/0.33/0.3

1205 Table 3: Mean change in climate and fluxes between 2002 and 2003 covering the period
1206 between June and September.

Site	Precipitation (mm month^{-1})	Air temperature (° C)	GPP (g C m^{-2} month^{-1})	LE (W m^{-2})
Tharandt	-115.57	1.45	-38.45	0.52
Hesse	-49.20	2.98	-123.38	-11.90
Roccarespampani	-87.36	2.18	-71.94	-6.17
Castelporziano	-20.31	4.57	-49.73	-6.47
Espirra	-14.45	1.77	28.46	22.83

1207

1208

1209

1210

1211

Table 4: Summary statistics of modelled and observed latent heat (LE) at the five FLUXNET sites during the main drought period (1st of June – 31st August, 2003). The results of the three parameterisations, which represent a spectrum of behaviour, ranging from high to low drought sensitivity, are shown for the three tested approaches (M1-M3) to obtain a weighted estimate of soil water potential (Ψ_S) across CABLE's soil layers. M1 uses a root-biomass weighted soil water content converted to Ψ_S, M2 calculates Ψ_S by integrated soil water content over the top 1.7m of the soil, and M3 is calculated using a dynamic weighting across soil layers. Sites have been ordered to show a mesic-xeric transition between sites (Tharandt to Espirra). For each site the best performing model simulation has been highlighted in bold.

Site	Ψ_S Method	Root Mean Squared Error (RMSE; W m^{-2})				Nash-Sutcliffe efficiency (NSE)				Pearsons's correlation coefficient (r)			
		CTRL	High	Medium	Low	CTRL	High	Medium	Low	CTRL	High	Medium	Low
Tharandt	M1	21.25	24.64;	26.57	29.55	-0.70	-1.28	-1.65	-2.28	0.69	**0.73**	**0.73**	0.70
	M2		34.59	36.20	36.97		-3.50	-3.93	-4.14		0.58	0.56	0.55
	M3		**25.90**	29.39	32.26		**-1.52**	-2.25	-2.94		0.72	0.67	0.63
Hesse	M1	28.50	36.22	41.59	51.49	0.15	-0.37	-0.81	-1.77	0.68	0.66	0.74	0.79
	M2		52.60	59.87	63.46		-1.89	-2.75	-3.21		0.80	0.75	0.71
	M3		**28.82**	45.32	56.46		**0.13**	-1.15	-2.33		0.79	**0.84**	0.77
Roccarespampani	M1	38.00	48.41	40.98	34.27	-0.34	-1.17	-0.55	-0.09	0.67	0.52	0.67;	0.81
	M2		31.62	22.81	26.81		0.08	0.52	0.34		0.83	0.84;	0.79
	M3		45.12	**18.27**	29.50		-0.88	**0.69**	0.20		0.67	**0.85**	0.81
Castelporziano	M1	31.76	38.77	40.54	40.40	-8.95	-13.82	-15.21	-15.10	0.18	-0.08	0.01	0.06

Espirra	M1	35.31	41.52	40.97	33.87	-3.35	-5.02;	-4.86	-3.01;	0.42	0.32	0.59	0.70
	M2		15.58	**13.82**	**13.84**		0.15;	**0.33**	**0.33**;		**0.77**	**0.74**	0.73
	M3		41.01	20.41	15.40		-4.81	-0.45	0.17		0.57	0.53	0.55

Table 5: Summary statistics of modelled and flux derived gross primary productivity (GPP) at the five FLUXNET sites during the main drought period (1st of June – 31st August, 2003). The results of the three parameterisations, which represent a spectrum of behaviour, ranging from high to low drought sensitivity, are shown for the three tested approaches (M1-M3) to obtain a weighted estimate of soil water potential (Ψ_S) across CABLE's soil layers. M1 uses a root-biomass weighted soil water content converted to Ψ_S, M2 calculates Ψ_S by integrated soil water content over the top 1.7m of the soil, and M3 is calculated using a dynamic weighting across soil layers. Sites have been ordered to show a mesic-xeric transition between sites (Tharandt to Espirra). For each site the best performing model simulation has been highlighted in bold.

Site	Ψ_S Method	Root Mean Squared Error (RMSE; g C m^{-2} d^{-1})				Nash-Sutcliffe efficiency (NSE)				Pearsons's correlation coefficient (r)			
		CTRL	High	Medium	Low	CTRL	High	Medium	Low	CTRL	High	Medium	Low
Tharandt	M1	2.06	2.27	**2.07**	2.10	0.33	0.19	**0.33**	0.31	0.80	**0.71**	0.66	0.61
	M2		2.25	2.29	2.30		0.20	0.18	0.17		0.52	0.51	0.50
	M3		2.23	2.12	2.20		0.22	0.30	0.25		0.66	0.59	0.55
Hesse	M1	2.85	3.57	**2.48**	2.94	0.48	0.18	**0.60**	0.44	0.79	0.78	0.78	0.71
	M2		2.65	3.22	3.47		0.55	0.33	0.22		0.75	0.67	0.62
	M3		3.51	2.71	3.24		0.21	0.53	0.32		**0.83**	0.75	0.66
Roccarespampani	M1	2.49	3.70	2.69	2.38	0.42	-0.28	0.32	0.47	0.85	0.64	0.82	0.87
	M2		2,12	**1.47**	2.84		0.58	**0.80**	0.24		**0.92**	0.91	0.87
	M3		3.74	1.73	3.08		-0.31	0.72	0.11		0.84	0.91	0.85
Castelporziano	M1	2.22	3.46	3.64	3.76	-2.16	-6.71	-7.51	-8.08	0.55	-0.18	0.07	0.13
	M2		2.65;	1.84	1.22		-3.52	-1.17	0.04		0.63	0.63	**0.81**
	M3		3.71	**0.95**	1.46		-7.82	**0.42**	-0.37		0.05	**0.81**	0.84
Espirra	M1	3.03	4.39	4.33	3.72	-2.67	-6.72	-6.51	-4.55	0.74	0.58	0.53	0.67

	M2	1.92	1.46	**1.34**	-0.48	0.14	**0.28**	0.80	**0.81**	**0.81**
	M3	4.70	2.01	1.43	-7.84	-0.62	0.18	0.34	0.74	0.78

1233

Figure 1

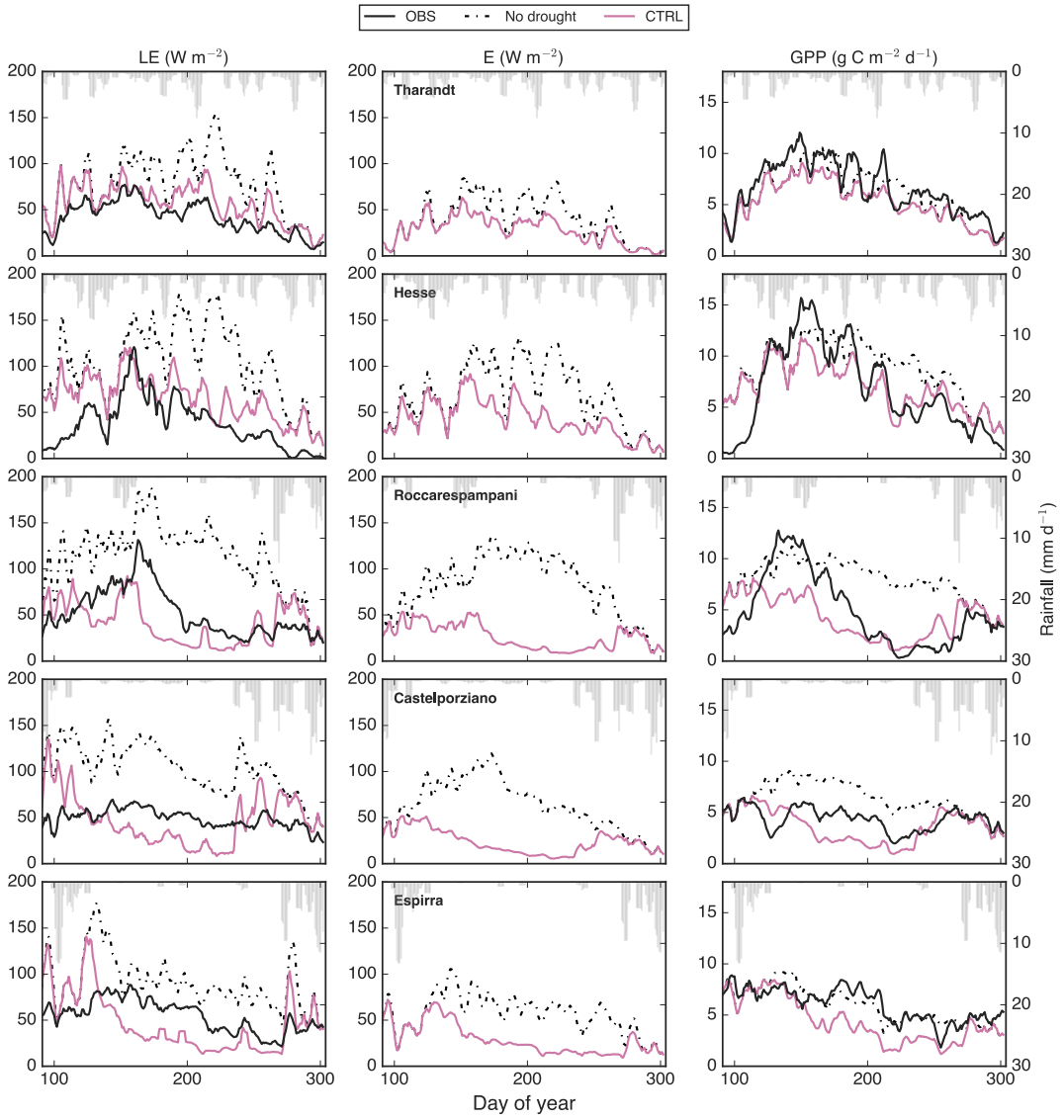
OBS
No drought
CTRL
LE (W m^{-2})
E (W m^{-2})
GPP (g C m^{-2} d^{-1})
Tharandt
Hesse
Roccarespampani
Castelporziano
Espirra
Rainfall (mm d^{-1})
Day of year

Figure 2

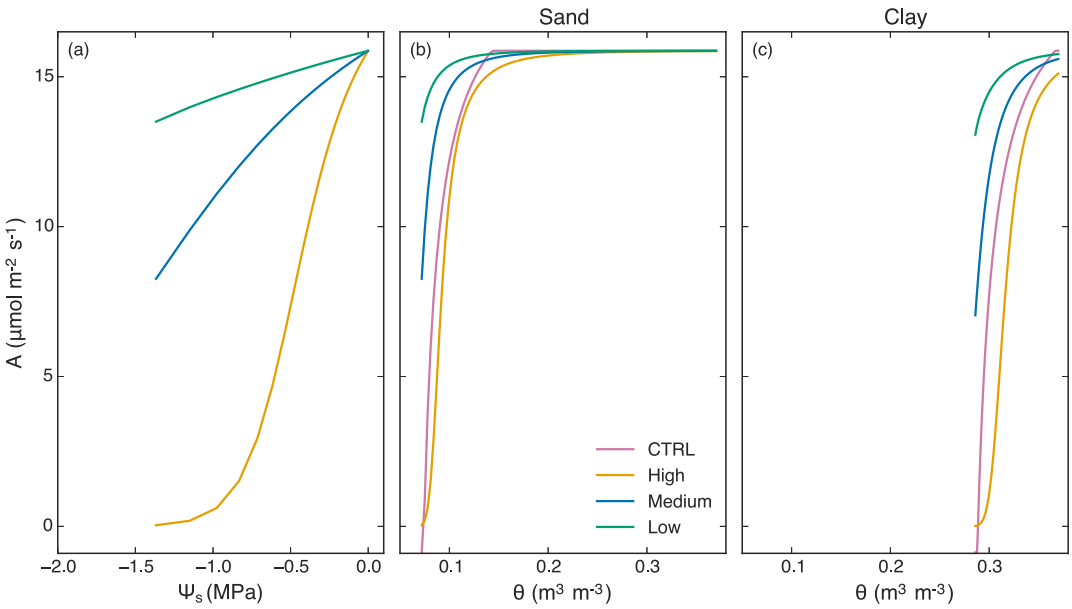
Sand
Clay
(a)
(b)
(c)
A (µmol m-2 s-1)
15
10
5
0
−2.0
−1.5
−1.0
−0.5
0.0
Ψs (MPa)
0.1
0.2
0.3
θ (m3 m-3)
CTRL
High
Medium
Low

Figure 3

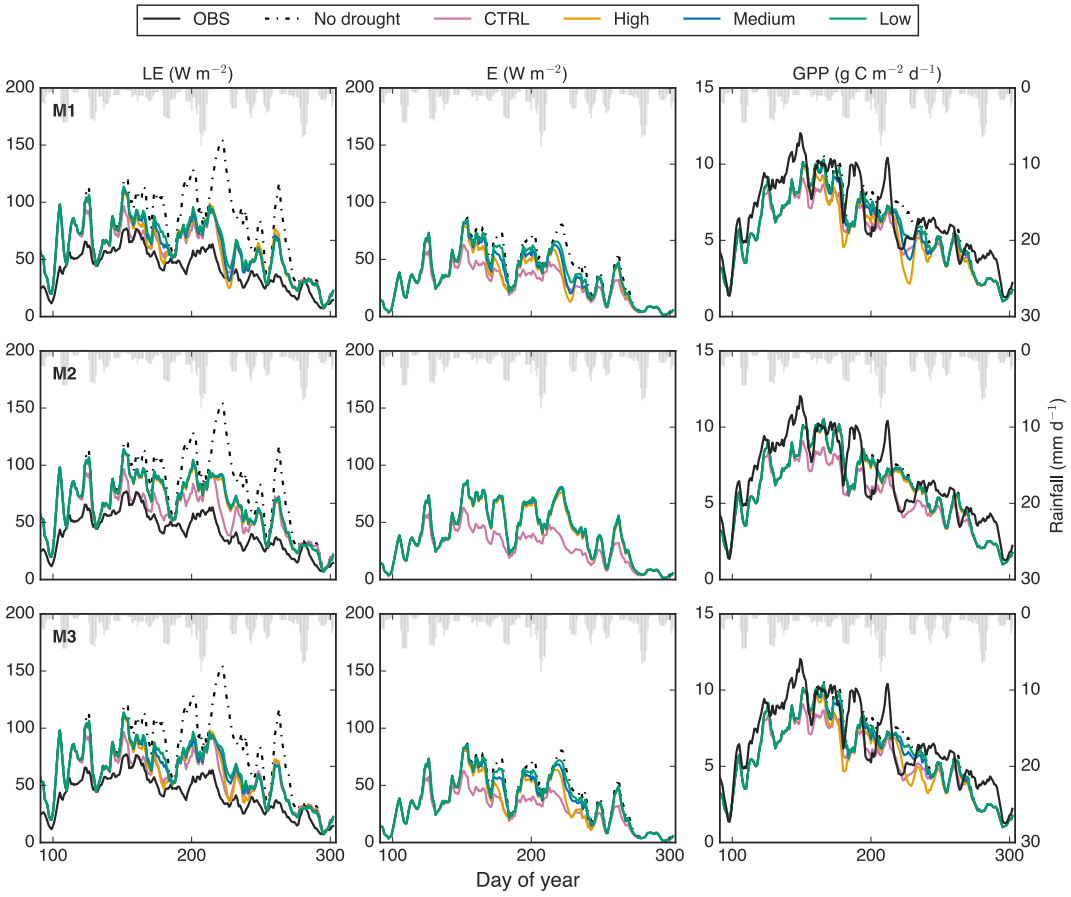
OBS
No drought
CTRL
High
Medium
Low
LE (W m^{-2})
E (W m^{-2})
GPP (g C m^{-2} d^{-1})
M1
M2
M3
Rainfall (mm d^{-1})
Day of year

Figure 4

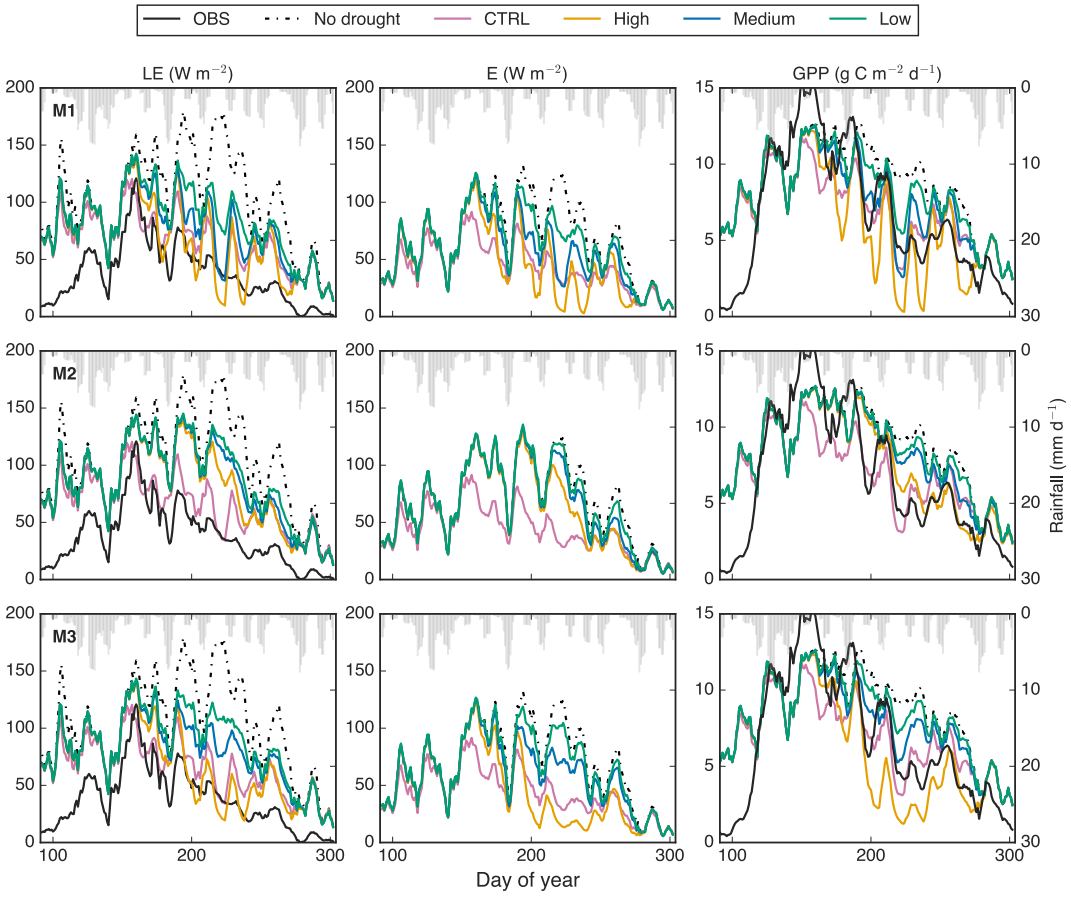
OBS
No drought
CTRL
High
Medium
Low
LE (W m^{-2})
E (W m^{-2})
GPP (g C m^{-2} d^{-1})
M1
M2
M3
Rainfall (mm d^{-1})
Day of year

Figure 5

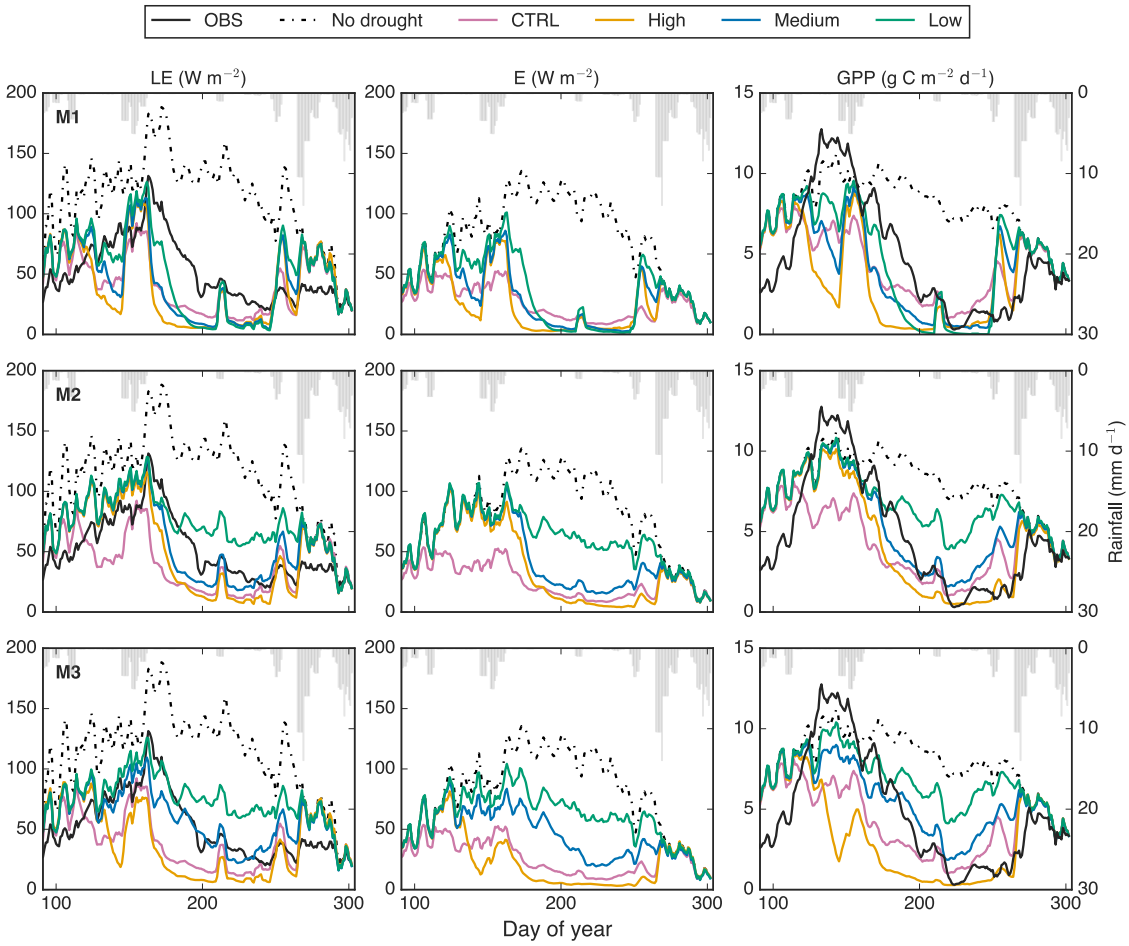
OBS
No drought
CTRL
High
Medium
Low
LE (W m^{-2})
E (W m^{-2})
GPP (g C m^{-2} d^{-1})
M1
M2
M3
Rainfall (mm d^{-1})
Day of year

Figure 6

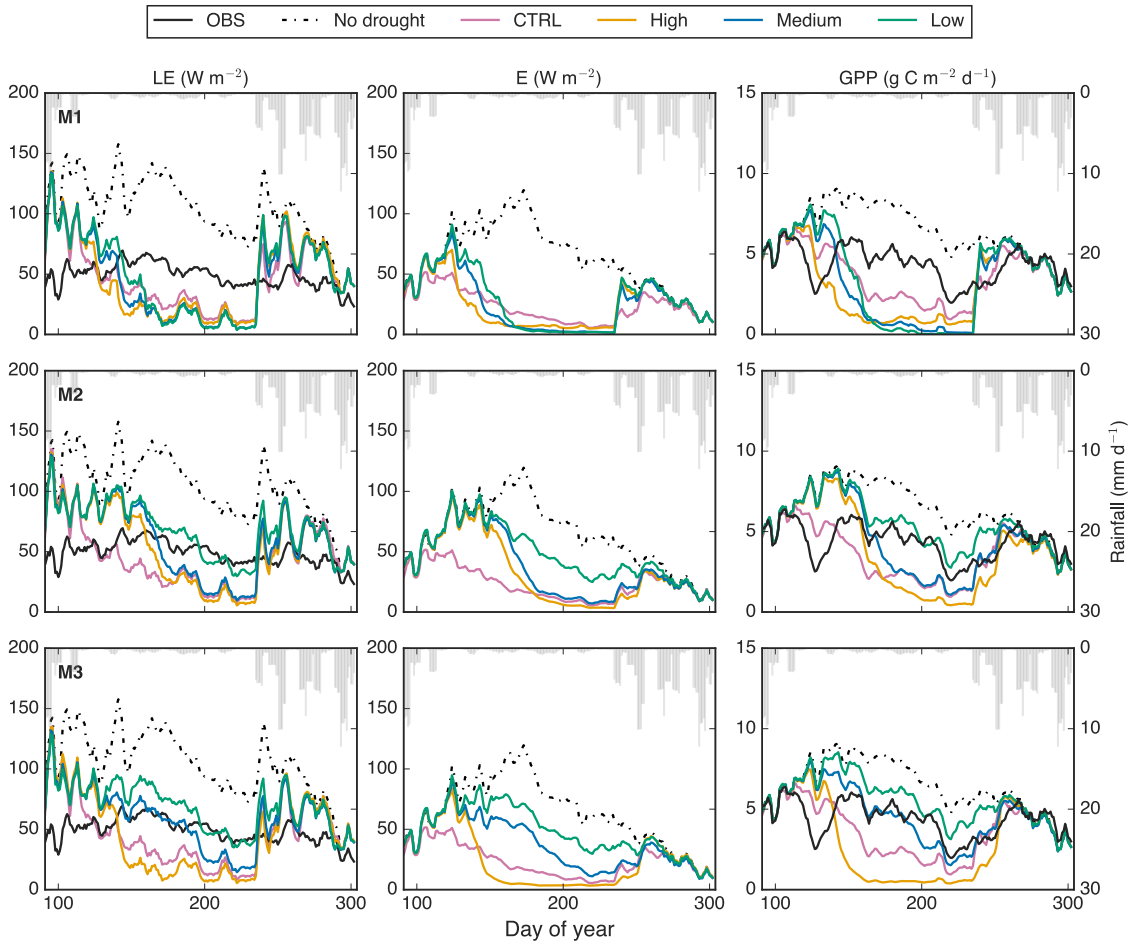
OBS
No drought
CTRL
High
Medium
Low
LE (W m^{-2})
E (W m^{-2})
GPP (g C m^{-2} d^{-1})
M1
M2
M3
Rainfall (mm d^{-1})
Day of year

Figure 7

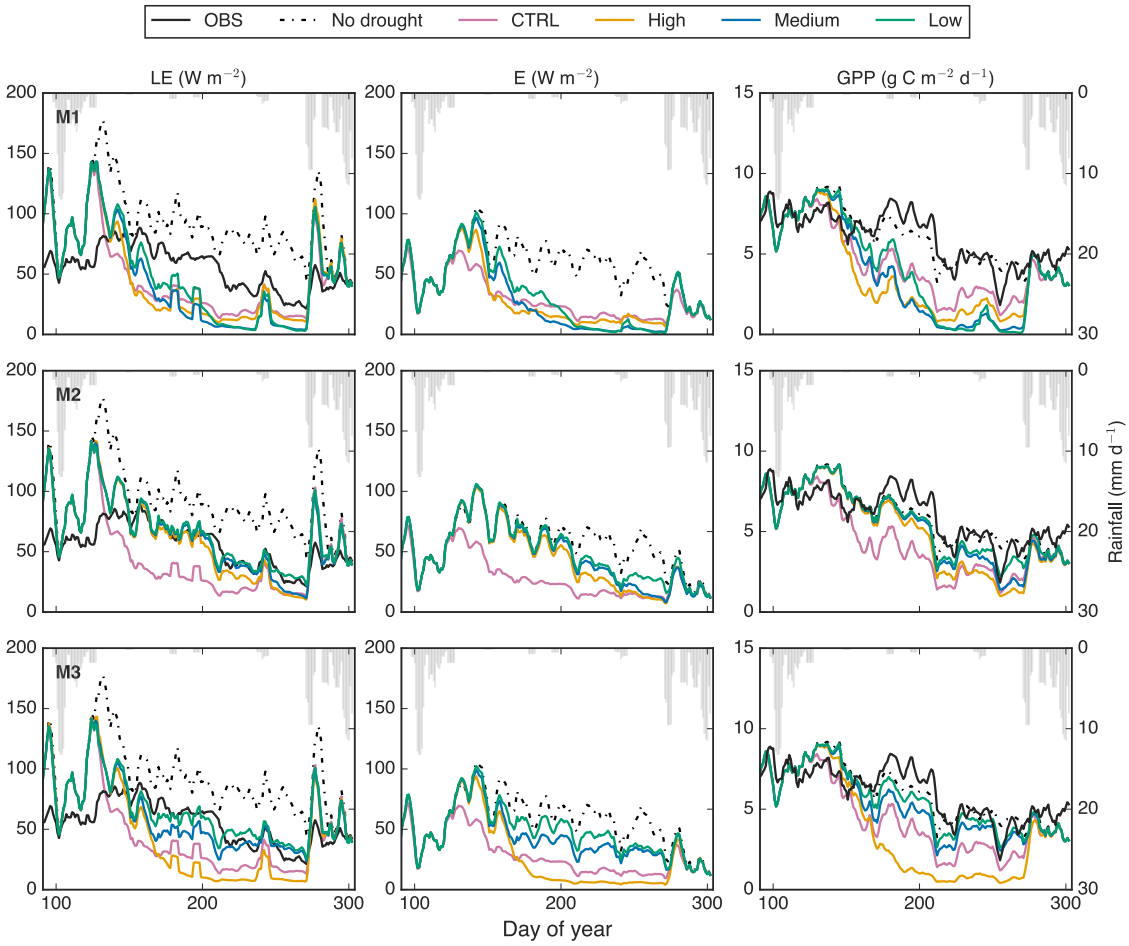
OBS
No drought
CTRL
High
Medium
Low
LE (W m^{-2})
E (W m^{-2})
GPP (g C m^{-2} d^{-1})
M1
M2
M3
Rainfall (mm d^{-1})
Day of year

Figure S1

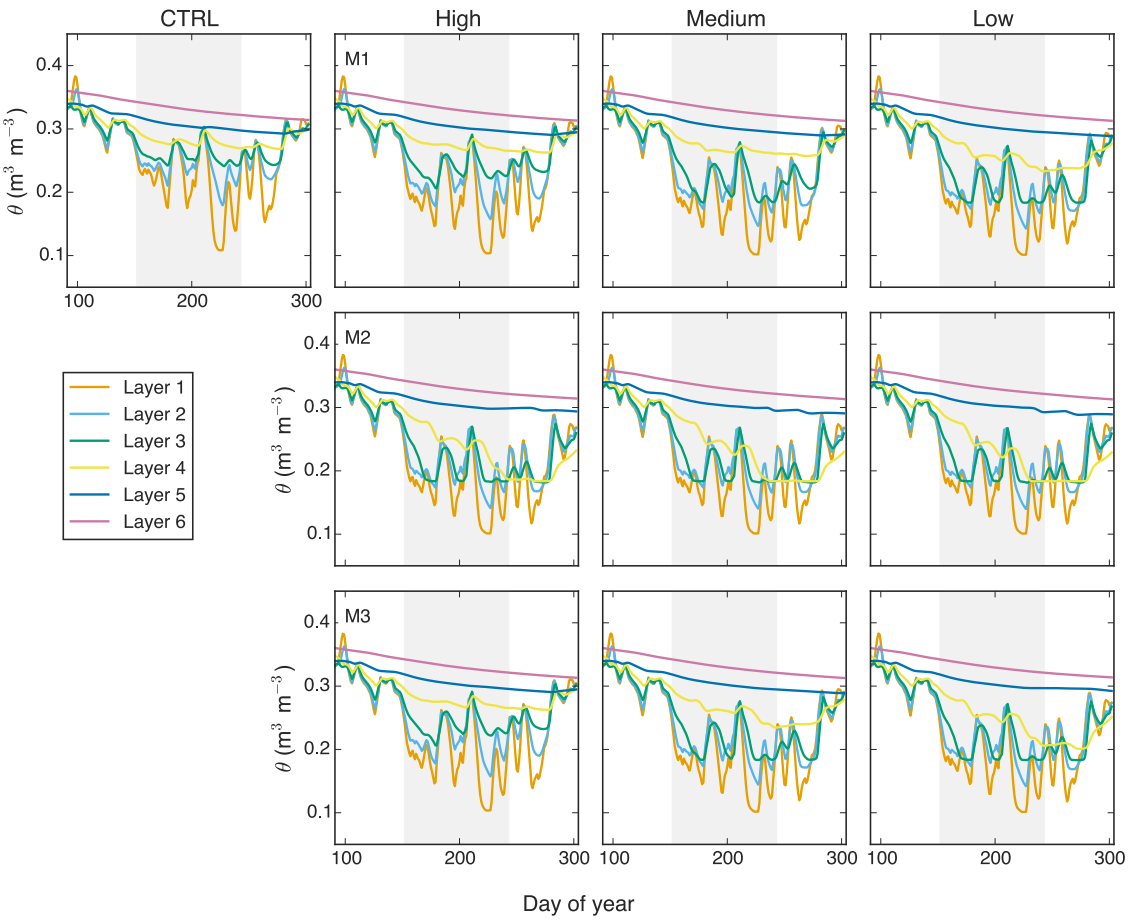
CTRL
High
Medium
Low
M1
M2
M3
θ (m³ m⁻³)
0.4
0.3
0.2
0.1
100
200
300
Layer 1
Layer 2
Layer 3
Layer 4
Layer 5
Layer 6
Day of year

Figure S2

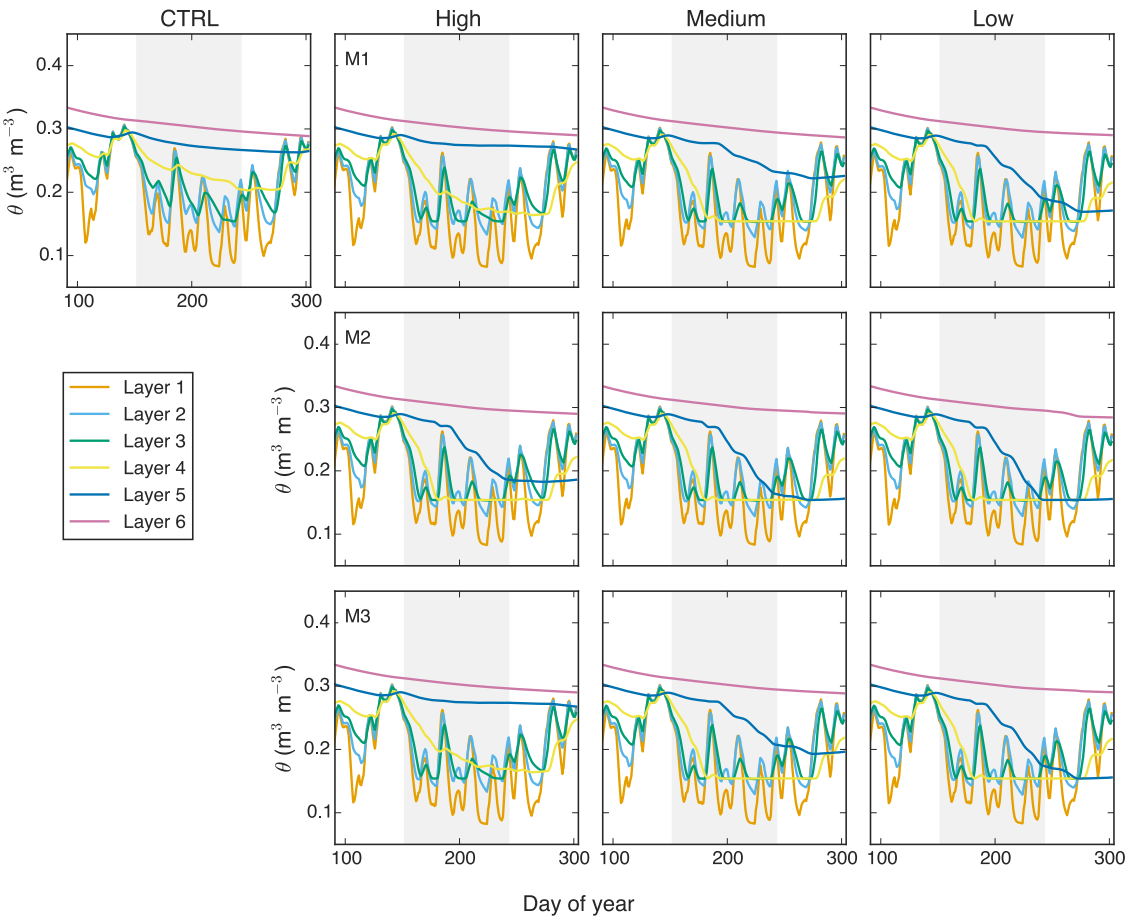
CTRL
High
Medium
Low
M1
M2
M3
θ (m³ m⁻³)
0.4
0.3
0.2
0.1
100
200
300
Layer 1
Layer 2
Layer 3
Layer 4
Layer 5
Layer 6
Day of year

Figure S3

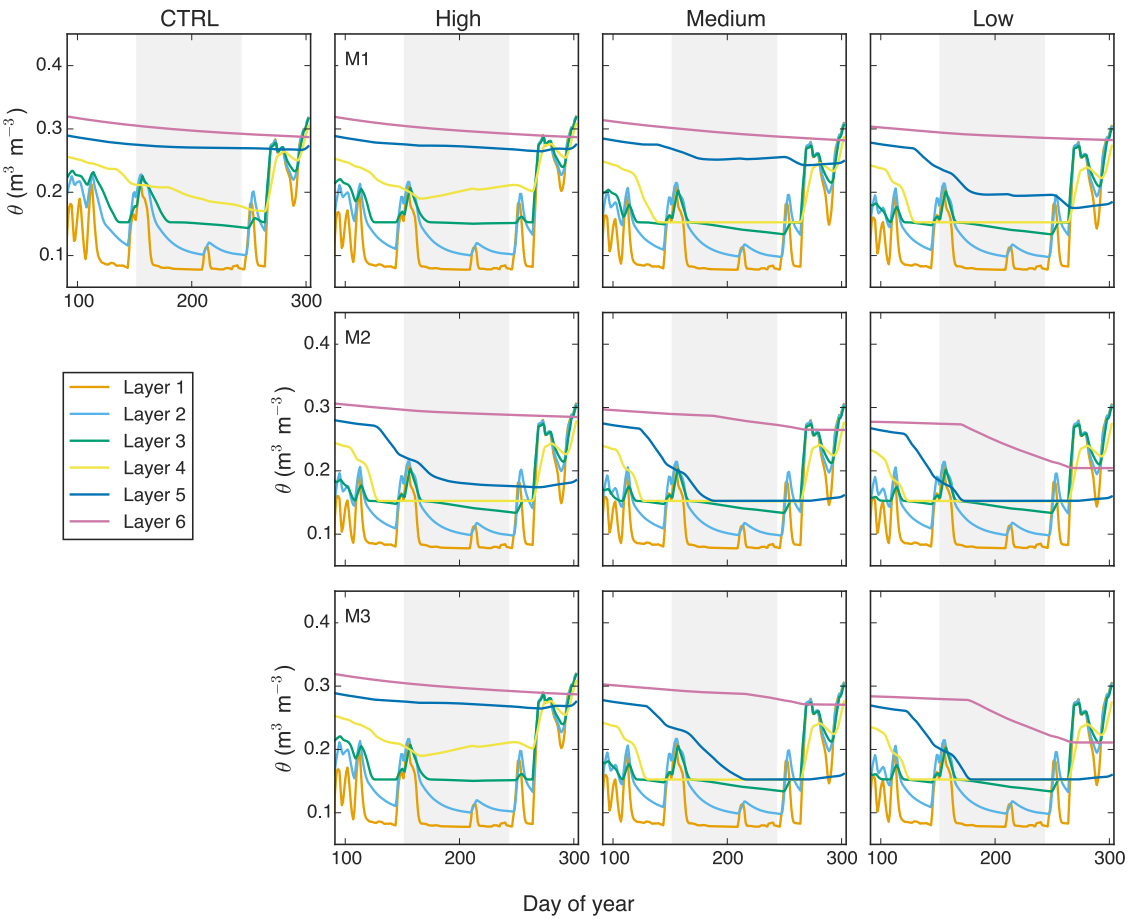
CTRL
High
Medium
Low
M1
M2
M3
θ (m³ m⁻³)
0.4
0.3
0.2
0.1
100
200
300
Layer 1
Layer 2
Layer 3
Layer 4
Layer 5
Layer 6
Day of year

Figure S4

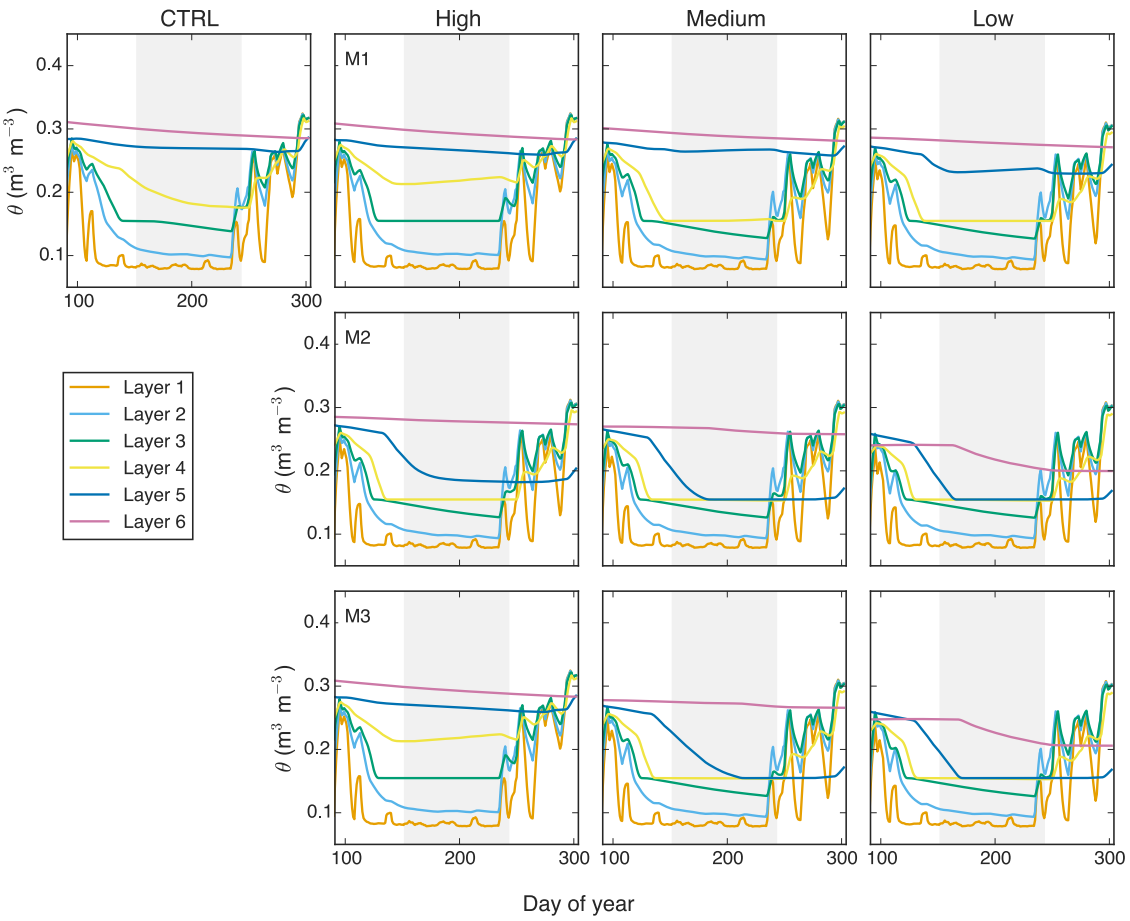
CTRL
High
Medium
Low
M1
M2
M3
θ (m³ m⁻³)
0.4
0.3
0.2
0.1
100
200
300
Layer 1
Layer 2
Layer 3
Layer 4
Layer 5
Layer 6
Day of year

Figure S5

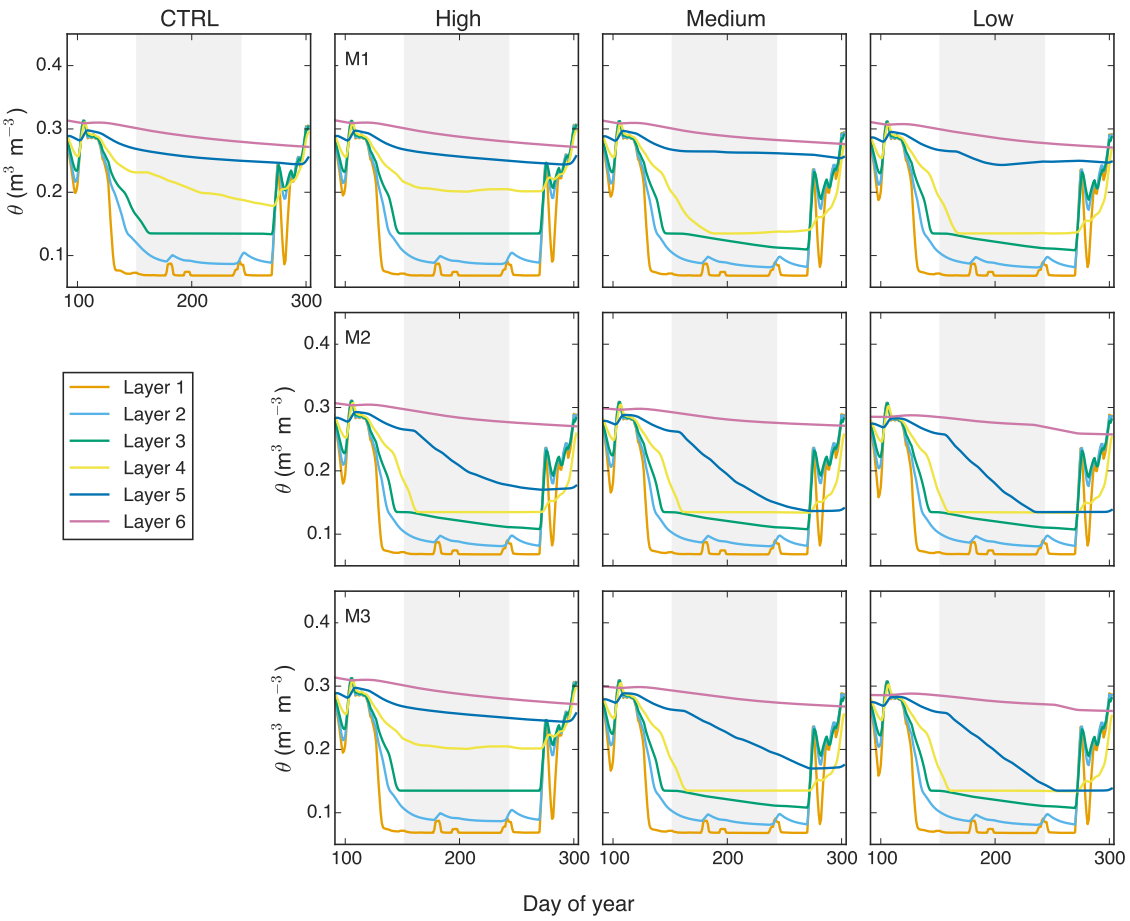
CTRL
High
Medium
Low
M1
M2
M3
θ (m³ m⁻³)
0.4
0.3
0.2
0.1
100
200
300
Layer 1
Layer 2
Layer 3
Layer 4
Layer 5
Layer 6
Day of year